Manitoba
Energy and Mines
Geological Services

Open File Report OF87-12

Preliminary Results of a Humus Geochemical Survey over the Rod Cu-Zn Deposit, Snow Lake, Manitoba

by K.J. Ferreira and M.A.F. Fedikow

Winnipeg, 1988

Energy and Mines

Hon. Jerry Storie
Minister

Charles Kang
Deputy Minister

Minerals Division

Sobharam Singh
Assistant Deputy Minister

Geological Services

W.D. McRitchie
Dirrector

TABLE OF CONTENTS

	Page
ABSTRACT	iv
INTRODUCTION	1
GEOLOGY	3
Regional Geology	3
Local Geology	3
SAMPLE COLLECTION, PREPARATION AND ANALYSIS	6
RESULTS	8
Manganese	10
Iron	11
Cobalt	12
Nickel	13
Copper	14
Zinc	15
Arsenic	16
Lead	17
Mercury	18
Specific Conductance	19
Hydrogen Ion	20
Summary	21
DISCUSSION	22
Future Work and Recommendations	22
CONCLUSIONS	23
ACKNOWLEDGMENTS	23
REFERENCES	24
APPENDIX I: Results of Analyzing Different Size Fractions for Representative Samples of Humus	25
APPENDIX II: Analytical Specifications	26
APPENDIX III: Raw Data	27
APPENDIX IV: Analytical Reproducibility	30
APPENDIX V: Histograms	32

TABLES

Table 1: Geometric characteristics of the Rod deposit. . . . 3
Table 2: Descriptive statistics. . . . 8
Table 3: Pearson correlation coefficient matrix. . . . 9
Table 4: Significant variable pairs based on Pearson correlation coefficients. . . . 9

FIGURES

Figure 1: General geology of the Flin Flon-Snow Lake greenstone belt. . . . 2
Figure 2: Geology of part of the Snow Lake area. . . . 4
Figure 3: Geology in the vicinity of the Rod Cu-Zn mine and location of the No. 1 and No. 2 Zones. 5
Figure 4: Sample locations. . . . 6
Figure 5: Contour diagram of Mn concentration in humus samples. . . . 10
Figure 6: Contour diagram of Fe concentration in humus samples. . . . 11
Figure 7: Contour diagram of Co concentration in humus samples. . . . 12
Figure 8: Contour diagram of Ni concentration in humus samples. . . . 13
Figure 9: Contour diagram of Cu concentration in humus samples. . . . 14
Figure 10: Contour diagram of Zn concentration in humus samples. . . . 15
Figure 11: Contour diagram of As concentration in humus samples. . . . 16
Figure 12: Contour diagram of Pb concentration in humus samples. . . . 17
Figure 13: Contour diagram of Hg concentration in humus samples. . . . 18
Figure 14: Contour diagram of *K* variation in humus samples. . . . 19
Figure 15: Contour diagram of H^+ concentration in humus samples. . . . 20

ABSTRACT

Sixty-six humus samples were collected from a grid overlying the deeply buried Rod Cu-Zn massive sulphide deposit to assess the applicability of humus geochemical exploration techniques in the Snow Lake greenstone belt. A 365 x 240 m multi-element geochemical anomaly, in proximity to the southwestern end of the Rod ore zone, was delineated on the basis of the variation in concentration of Cu, Zn, Co, Ni, Fe, Mn, *K* and H^+. This anomaly was recognized despite burial of the southwestern end of the ore zone beneath 1-6 m of variable overburden and an additional 183 m of bedrock. No geochemical response was obtained over the more deeply buried (732 m) east end of the ore zone. Conductivity values, expressed in terms of specific conductance (*K*), form anomalies that are correlative in location and magnitude of response to the Cu, Zn, Ni, Co, Fe and Mn anomalies in the humus. H^+ contents of the humus delineate a low contrast anomaly that correlates with the multi-element geochemical anomaly as well as with single element anomalies apparently unrelated to the Rod mineralization.

These results suggest that the rapid, cheap and non-destructive determination of *K* and H^+ in humus samples may be useful in prescreening large survey areas and reducing these to more localized areas where routine, effective, but more costly exploration techniques such as geophysical surveys and diamond drilling can be undertaken. Specific conductance and hydrogen ion concentrations should be determined upon completion of sampling; subsequent analysis of the anomalous humus samples for base and precious metals could then confirm and categorize "base metal" or "precious metal" targets. This procedure will reduce the total number of chemical determinations, and therefore the analytical costs, by reducing the total sample population to those samples reflecting anomalous *K* and H^+.

INTRODUCTION

An examination of geochemical exploration techniques is currently being undertaken in the Snow Lake area as part of mineral deposit programming under the Canada-Manitoba Mineral Development Agreement. The Rod Cu-Zn deposit humus geochemical survey was initiated to test humus geochemical response over a known, deeply buried massive sulphide-type deposit and to determine chemical elements diagnostic of the Rod deposit. A rock geochemical study covering the same area will be the subject of another Manitoba Energy and Mines Open File Report.

Humus surveys represent one of the more widely used biogeochemical prospecting methods particularly in areas of limited exposure. Trace elements, liberated from weathered minerals, are dispersed in soil, absorbed as plant nutrients, and redeposited in the soil profile by decaying vegetation. The distribution of these elements may assist in locating mineralized and altered zones.

Govett (1976) concluded that the concentration of hydrogen ions could be a sensitive indicator of deeply buried sulphide deposits. To test this type of geochemical response at the Rod deposit, pH and conductivity measurements were made in addition to the more routine trace element analyses.

A total of 66 humus (A1) samples were collected at 200 ft. (61 m) spacings on a referenced grid cut for exploration purposes. The location of the surface infrastructure of the Rod mine precluded complete coverage of the sampling area.

This report presents the data derived from this survey and discusses the ability of Mn, Co, Ni, Cu, Zn, Mo, As, Sb, Pb, Hg, Bi, Fe, Ag, H^+ concentrations, and conductivity to indicate the presence of deeply buried mineralization in this area.

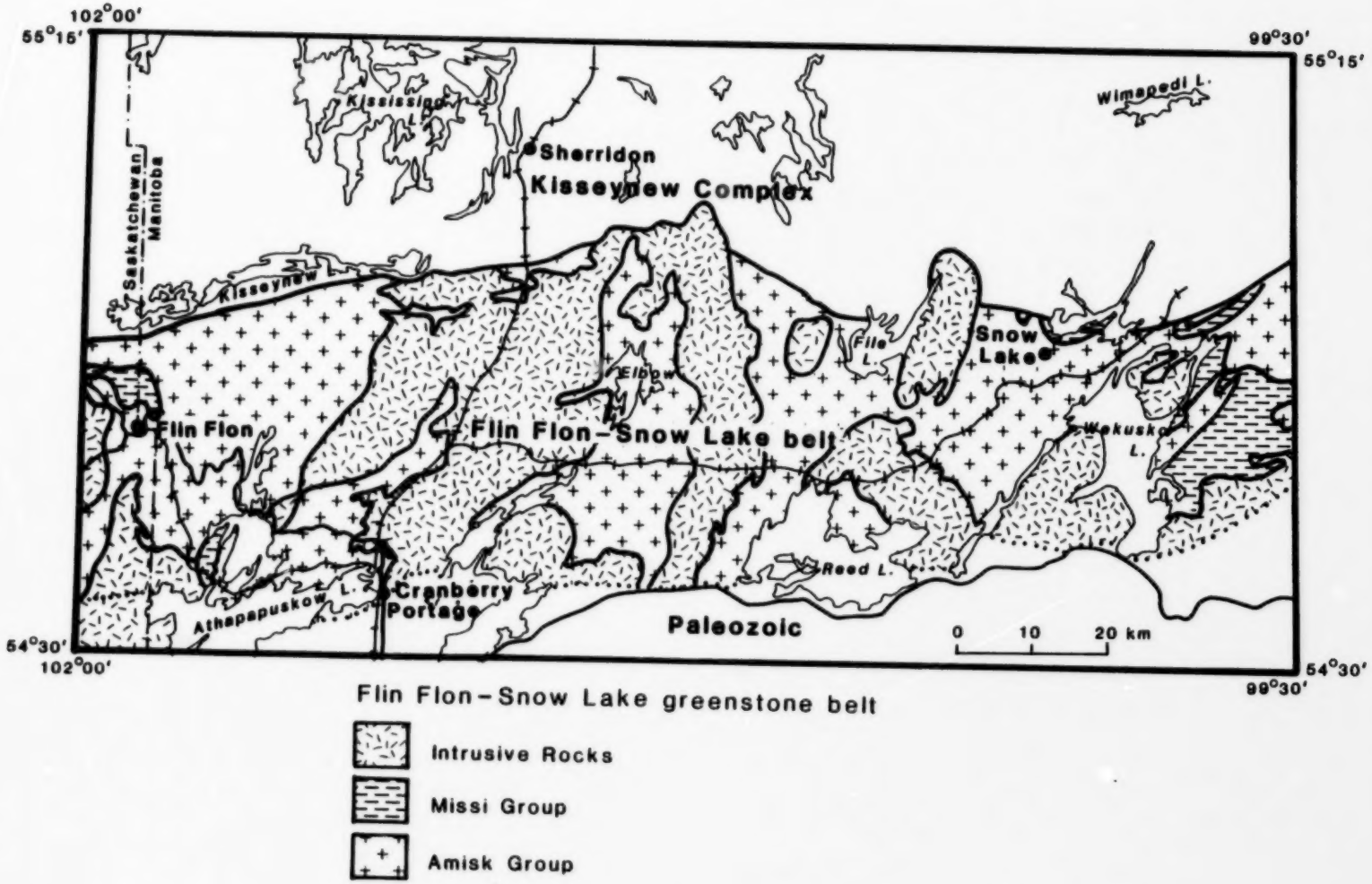

Figure 1: General geology of the Flin Flon-Snow Lake greenstone belt.

GEOLOGY

Regional Geology

The Flin Flon-Snow Lake greenstone belt comprises Proterozoic metamorphosed volcanic, sedimentary, and intrusive rocks (Fig. 1). The belt extends 250 km in length with an exposed width of 32 to 48 km (Bailes et al., 1987). The greenstone belt, part of the southern Churchill Province, is bounded by the Kisseynew sedimentary gneiss belt to the north and unconformably overlain by Ordovician dolomitic limestones to the south.

The volcanic and associated sedimentary rocks were assigned to the Amisk Group by Bruce (1918). Subaqueous and subaerial depositional environments have been identified. Basaltic to rhyolitic flows, pyroclastic and volcaniclastic rocks are present as well as minor iron formation, conglomerate, and other epiclastic sedimentary rocks. The Snow Lake portion of the greenstone belt contains abundant felsic volcanic rocks and volcanogenic greywacke turbidites; hydrothermal alteration affected large areas of the felsic rocks (Bailes et al., 1987).

Younger clastic rocks, assigned to the Missi Group by Bruce (1918), include sandstones and conglomerates that were generated in a fluvial-alluvial environment (Bailes et al., 1987). In the Snow Lake area the Missi Group also contains some subaerial and subaqueous volcanic rocks (Bailes et al., 1987).

An isoclinal folding event (F1), a second folding event (F2) with northeast-trending axial traces and the formation of gneiss domes have affected rocks in the Snow Lake area (Froese and Moore, 1980). Two major faults, the early McLeod Road thrust fault and the late Berry Creek fault, and minor smaller fractures and shear zones are present (Froese and Moore, 1980). Rocks in the Snow Lake area attained lower to upper amphibolite facies metamorphism (Bailes et al., 1987; Froese and Moore, 1980).

Local Geology

The Rod volcanogenic Cu-Zn deposit is located in the Aphebian (?) Snow Lake area (Fig. 2). Owned by Falconbridge Ltd. (50%) and Stall Lake Mines Ltd. (50%), it is currently leased to Hudson Bay Mining & Smelting Co. Production and reserve estimates total 688 000 tonnes of 7.2% Cu and 3.0% Zn with minor gold and silver (Esposito, 1986). Production began in 1984, after an exploration history that dates to 1951 and includes Cu-Zn production from 1962-1964 from the smaller No. 1 Zone by Stall Lake Mines Ltd.

Overburden at the Rod deposit includes a sphagnum moss layer 20-25 cm thick overlying the humus layer. The brownish-black humus layer containing decomposed vegetation is up to 13 cm thick and is underlain by 1-6 m of a variety of dense grey clay, mixed clay and silt, and brown oxidized till (?) overlying bedrock. The ore zone is at a depth of 183 m along L96W and 732 m along L72W.

The Rod deposit occurs near the crest of the Anderson Lake anticline, an isoclinal F1 fold (Froese and Moore, 1980). It occurs within the quartz-phyric uppermost 100 m of the Lower Mine felsic unit that is composed of intercalated felsic and mafic flows and pyroclastic rocks of the central part of the Amisk Group (Bailes et al., 1987). The Stall, Ram, Linda and Anderson Cu-Zn massive sulphide-type deposits are situated in similar stratigraphic and structural environments (Froese and Moore, 1980). Rocks enclosing the Rod deposit include mafic flows and pyroclastic rocks, felsic pyroclastic rocks, and quartz porphyry (Fig. 3). Carbonatization is ubiquitous in the mineralized zone, the hanging wall and, to a lesser extent, in the footwall of the deposit (Coats et al., 1970).

The Rod deposit consists of two zones, the No. 1 Zone that was mined by Stall Lake Mines Ltd. from 1962-1964, and the larger No. 2 Zone that was delineated by exploration activity beginning in 1965 (Fig. 3) and is the current base of exploitation. This study was conducted over the No. 2 Zone and all references to the Rod deposit will refer to the No. 2 Zone unless otherwise noted. Table 1 describes the geometry of the linear plunging deposit.

The average sulphide content in the massive sulphide zone is: chalcopyrite, 40%; pyrite, 30%; sphalerite, 15%; pyrrhotite, 12%; arsenopyrite, 3%; with minor galena, marcasite, gold and silver (Coats et al., 1970).

The sulphide-bearing zone has a total apparent width of 120 to 245 m. It consists of a massive sulphide zone that changes laterally to a zone of lower grade disseminated sulphide mineralization (Coats et al., 1970). Contacts between the sulphide zone and wall rocks are very sharp perpendicular to the plane of the sulphide zone (op. cit.).

TABLE 1: GEOMETRIC CHARACTERISTICS OF THE ROD DEPOSIT (NO. 2 ZONE)
(FROM COATS ET AL., 1970)

Plunge:	N25E/25°-35°
Dip:	50-60°NW
Thickness:	3.65 m
Width:	46-61 m
Length:	
Plan length (vertical projection) = 533 m	
Plunge length (between 500' and 1500' elevations) = 625 m	
Vertical Depth to Orebody:	
Southern end = 183 m	
Northern end = 732 m	

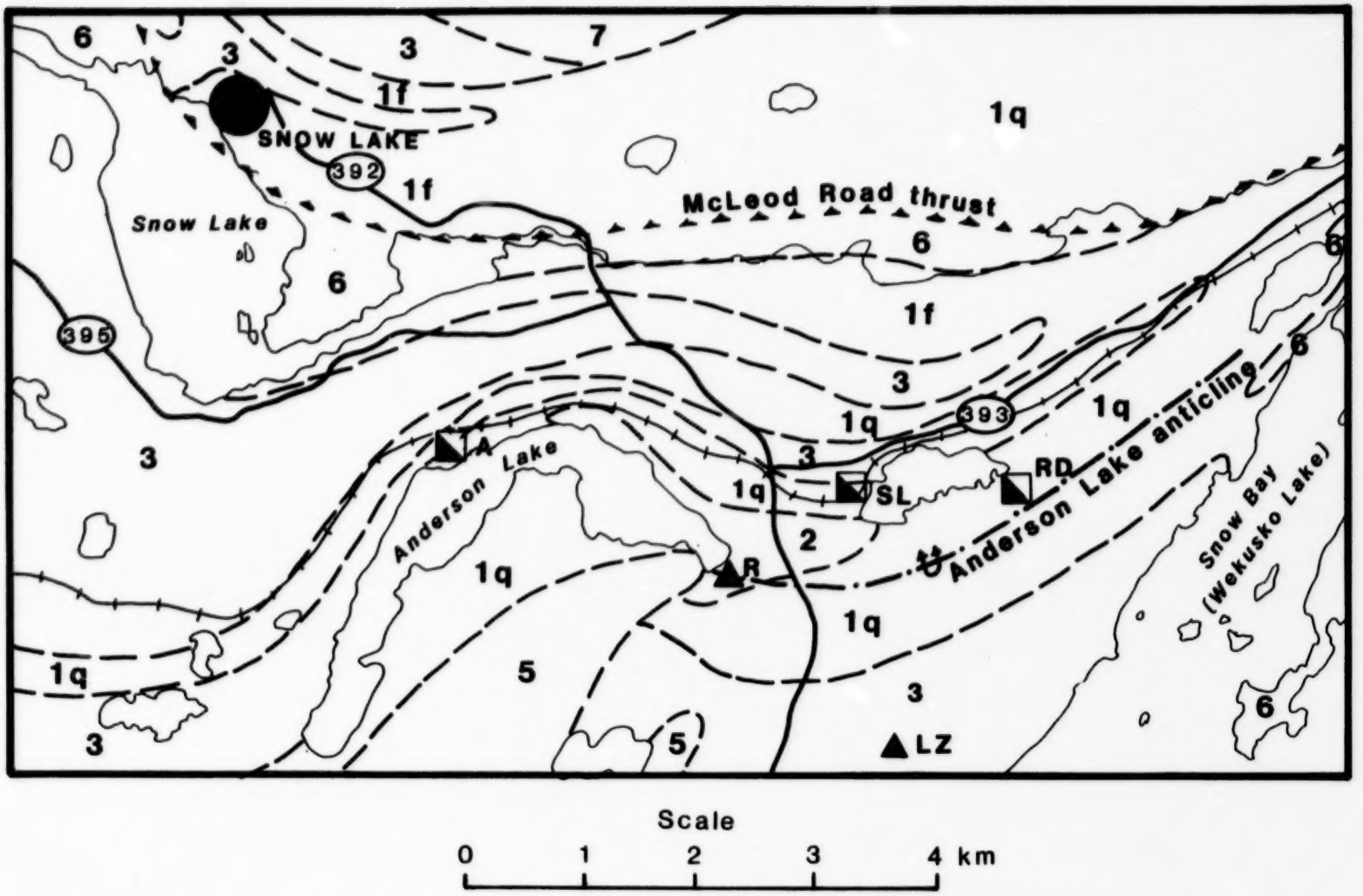

Figure 2: Geology of part of the Snow Lake area. Amisk Group: 1 - Felsic pyroclastic and volcaniclastic rocks; q) quartz-eye; f) fragmental; 2 - Altered volcanic rocks of Unit 1; 3 - Mafic lavas, pyroclastic and volcaniclastic rocks; 5 - Quartz-eye tonalite; 6 - Greywacke and shale. Missi Group: 7 - Lithic arenite. A - Anderson Lake Cu-Zn mine; RD - Rod Lake Cu-Zn mine; SL - Stall Lake Cu-Zn mine; LZ - Linda Zone Cu-Zn deposit; R - Ram Zone Cu-Zn deposit (after Froese and Moore, 1980).

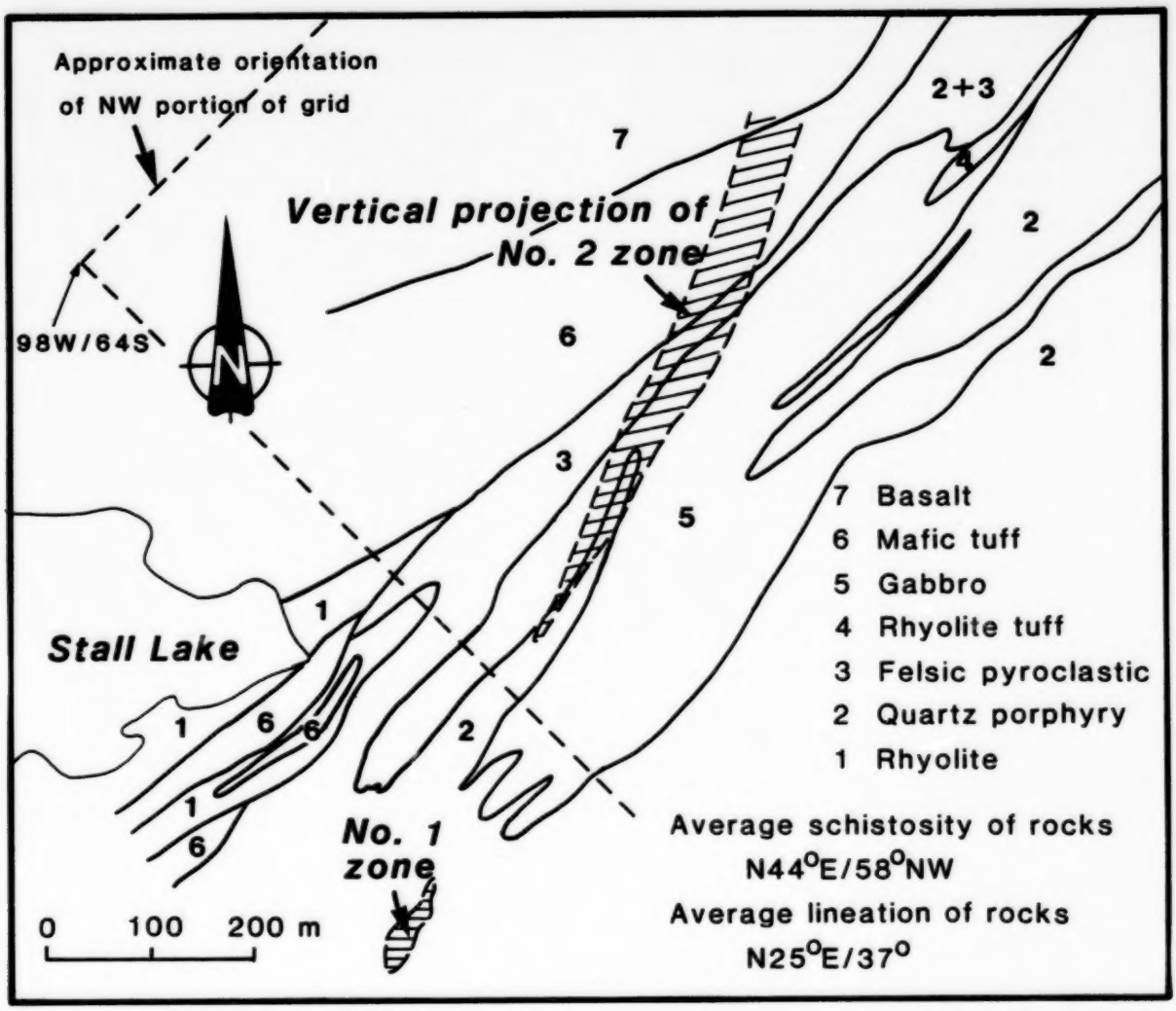

Figure 3: Geology in the vicinity of the Rod Cu-Zn mine and location of the No. 1 and No. 2 Zones (after Coats et al., 1970).

SAMPLE COLLECTION, PREPARATION AND ANALYSIS

Sixty-six humus samples were collected along a cut grid over the Rod mine. Line spacings were usually 400 ft. (122 m) with sample stations located at 200 ft. (61 m) intervals, reduced to 100 ft. (30.5 m) intervals over the vertical projection of the ore zone (Fig. 4). The sample locations correspond to the sites where Aurex Hg-gas detector cups had been implanted in 1985 (Fedikow, 1986a). These holes, approximately 25-45 cm deep, were dug to the permafrost level. For the humus survey, the mercury gas survey holes were located and humus was collected from them by hand to fill white cotton sample bags (19 x 27 cm).

The samples were air-dried in the field to avoid on-going biological activity and modification of pH, further dried in a low temperature oven (45°C) and sieved to -80 mesh. Attempts were made to concentrate and analyze the less than 2 micron size fraction but the samples usually lacked sufficient material in this size range. Only

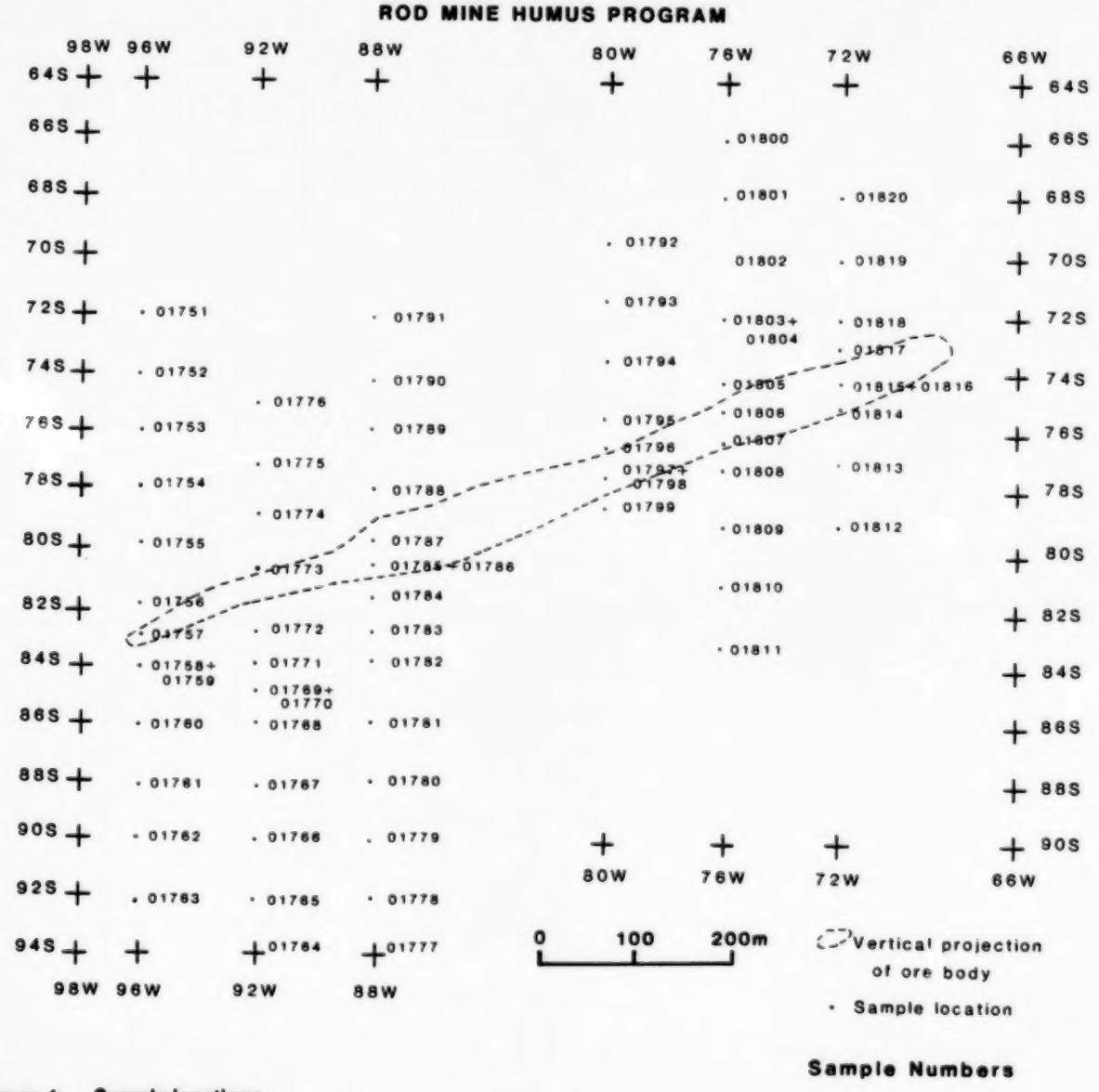

Figure 4: Sample locations.

one sample (1794) in a test batch bore sufficient amounts of material in both the -80 mesh and the less than 2 micron size fractions to enable a comparison. For this sample there were significant differences in concentration among elements between the two size fractions: the less than 2 micron size fraction yielded substantially lower concentrations of Mn, Zn and Mo, but higher values for Fe, Pb and Cu (Appendix I).

A 0.50 g homogenized representative split was digested in hydrochloric and nitric acids (1:3). Analysis for Mn, Fe, Co, Ni, Cu, Zn, As, Mo, Ag, Sb, Pb and Bi by DC Plasma was done by atomic absorption spectrophotometry. Hg was determined by cold vapour atomic absorption spectrophotometry after an HNO_3-H_2SO_4-HCl-$HMnO_4$ extraction. Lower limits of detection are: 1 ppm for Mn, Co, Ni, Cu, Zn and Mo; 5 ppm for As, Sb and Pb; 5 ppb Hg; 2 ppm Bi; 0.1% Fe, and 0.5 ppm Ag. Analyses were performed by Bondar-Clegg & Co. Ltd., Ottawa.

For the measurement of conductivity and pH a 0.50 g representative sample of the -80 mesh size fraction was suspended in 100 ml of deionized water. This slurry was tested for conductivity using a Radiometer conductivity meter (Type CDM2e) and electrode (Type CDC104) and for pH using a Fisher Accumet pH meter model 620, a Fisher universal glass pH electrode (#13-639-3) and a Fisher Calomel reference electrode (#13-639-62). These measurements were made by Manitoba Energy and Mines Analytical Laboratory, Winnipeg.

Analytical specifications are summarized in Appendix II and raw data are presented in Appendix III. Duplicate samples collected from the same sampling locations at the same time yield an average analytical reproducibility of ±23% (Appendix IV). Examination of these statistics reveals that sample number pairs 1815 + 1816 and 1758 + 1759 are responsible for most of the spurious results. Mn and, to a lesser degree, Co and Zn are inconsistent among the individual elements, yielding reproducibilities ranging from ±2% to ±90%. The duplicate sample pairs were re-analyzed at Manitoba Energy and Mines Analytical Laboratory, Winnipeg; analyses were comparable to those obtained for the same samples at Bondar-Clegg & Co. Ltd. (Appendix IV). Thus, the discrepancies are not due to analytical error, but are probably due to differences in concentration in the sampling medium itself or contamination of samples by other parts of the soil profile at the time of sampling. Considering the size of sample that was necessary to be collected to provide two duplicate samples, and the comparatively small size of a hole that was available to be sampled by hand without the aid of tools, the possibility of contamination must be considered. The placement and the general level of contrast of anomalies is little affected by differences in reproducibilities, i.e., if a duplicate sample pair has markedly different Cu values, both values will still be anomalously high, both will have background values, or both will be anomalously low.

RESULTS

Histograms of the geochemical data for each element analyzed are presented in Appendix V. Descriptive statistics for Mn, Fe, Co, Ni, Cu, Zn, As, Pb, Hg, *K* and H^+ are presented in Table 2. Statistics for As should be interpreted with caution because all but nine of the 66 analyses are below the limits of detection (5 ppm As). Mo, Ag, Sb, and Bi are ineffective in this survey, yielding either values that are below analytical detectibility limits or that have ranges that are too small to discriminate anomalies; no further consideration is given to these elements.

The skewness and kurtosis statistics in Table 2 show distributions that are highly peaked and positively skewed. This distribution indicates the presence of multiple populations within the data set, those being (i) low concentration or background values and (ii) elevated concentrations or anomalous values. Variance and standard deviation, measures of dispersion within the sample set, will increase if the data set does not approximate normal distribution. Thus, the presence of data subsets with background and anomalous concentration will yield a set of analyses with large variance and standard deviation statistics. Mn, Zn, Hg, Cu and *K* are the variables with the greatest observed variance, although most elements in this study exhibit sizeable dispersion statistics (Table 2).

A Pearson nonparametric correlation coefficient matrix for the data set is presented in Table 3 with a sum-

TABLE 2: DESCRIPTIVE STATISTICS, HUMUS SAMPLES,

ROD CU-ZN DEPOSIT

Element	Arithmetic Mean	Median	Mode	Minimum Value	Maximum Value	Standard Deviation	Variance	Skewness	Kurtosis
Mn, ppm	1196	577	437	15	17140	2380	5663706	5.154	31.828
Fe, %	1.1	0.9	0.4	0.1	3.8	0.8	0.6	1.204	1.372
Co, ppm	16	6	4	1	166	29	832	3.854	16.250
Ni, ppm	14	9	7	1	83	16	264	2.657	6.929
Cu, ppm	79	54	28	9	487	85	7286	3.076	10.906
Zn, ppm	178	87	37	14	1236	270	72983	2.879	7.561
As, ppm[1]	121	42	14	13	434	164	27037	1.543	0.734
Pb, ppm	29	28	14	6	81	14	190	1.393	3.656
Hg, ppb	161	128	125	20	1110	141	19976	4.947	31.594
K, micro-mhos/cm	41	24	12	2	183	41.9	1753	1.918	3.634
H^+, ppm	4.6	0.7	8.3	0.03	55	9.3	87.2	3.637	15.221

[1] Statistics based upon 9 analyses; 57 analyses below the analytical limit of detection (5 ppm)

TABLE 3: PEARSON CORRELATION COEFFICIENT MATRIX, HUMUS SAMPLES, ROD CU-ZN DEPOSIT, 99% LEVEL OF CONFIDENCE

	Mn	Fe	Co	Ni	Cu	Zn	As	Pb	Hg	*K*	H^+
Mn	1.0000	0.1250	0.4541*	0.3700	0.2308	0.5071*	0.0368	0.1991	0.1176	0.2914	-0.2001
Fe	0.1250	1.0000	0.3004	0.2920	0.3708	0.2369	0.1756	0.3206	-0.2211	-0.0620	-0.3410
Co	0.4541*	0.3004	1.0000	0.8841*	0.7709*	0.8446*	0.0559	0.1434	-0.0812	0.4987*	-0.1522
Ni	0.3700	0.2920	0.8841*	1.0000	0.7108*	0.8945*	-0.0113	0.1857	-0.0950	0.5668*	-0.2022
Cu	0.2308	0.3708	0.7709*	0.7108*	1.0000	0.6041*	0.0487	0.1650	-0.0895	0.3737*	-0.1878
Zn	0.5071*	0.2369	0.8446*	0.8945*	0.6041*	1.0000	0.0401	0.1447	-0.0355	0.5487*	-0.1942
As	0.0368	0.1756	0.0559	-0.0113	0.0487	0.0401	1.0000	0.1401	0.0456	0.1093	-0.0910
Pb	0.1991	0.3206	0.1434	0.1857	0.1650	0.1447	0.1401	1.0000	0.1067	-0.0277	-0.3099
Hg	0.1176	-0.2211	-0.0812	-0.0950	-0.0895	-0.0355	0.0456	0.1067	1.0000	-0.0252	-0.0176
K	0.2914	-0.0620	0.4987*	0.5668*	0.3737*	0.5487*	0.1093	-0.2770	-0.0252	1.0000	-0.0893
H^+	-0.2001	-0.3410	-0.1522	-0.2022	-0.1878	-0.1942	-0.0910	-0.3099	-0.0176	-0.0893	1.0000

Note: Coefficients marked by an asterisk are considered significant at a 99% level of confidence.

mary of statistically significant variable pairings listed in Table 4. These represent pairs of data points for which a significant linear relationship exists at the 99% confidence level. Mo, Ag, Sb and Bi have been omitted from the matrix, and caution is again advised in interpreting the role of As in these correlations. Strong correlations among Cu, Zn, Ni, and Co reflect the association of those elements that form the sulphide minerals present in the area. Fe, however, does not appear to be as correlative with this group of elements despite the dominance of pyrite and pyrrhotite in the sulphide mineralogy of the area of the Rod deposit. The high correlation coefficient of specific conductance (*K*) and Cu, Zn, Ni, and Co is notable. Since specific conductance is a measure of the concentration of ions in solution, the presence of anomalous concentrations of cations should be reflected in a concomitant increase in conductivity.

Contour diagrams are used to examine the variation in values for individual elements and the placement of anomalies relative to the vertical projection of the ore zone. Contour intervals were determined upon visual inspection of the individual data sets. A graphical determination of threshold value described by Tennant and White (1959) was considered but rejected for this study: multiple data populations within a data set may lead to less than useful, if not inaccurate, threshold determinations (Fedikow, 1986a; Fedikow and Ferreira, 1987). References to location will be made with respect to grid direction rather than compass direction.

TABLE 4: SIGNIFICANT VARIABLE PAIRS BASED ON PEARSON CORRELATION COEFFICIENTS AT THE 99% CONFIDENCE LEVEL, HUMUS SAMPLES, ROD CU-ZN DEPOSIT

Co - Mn	Cu - Zn
Co - Ni	Mn - Zn
Co - Cu	*K* - Co
Co - Zn	*K* - Ni
Cu - Ni	*K* - Cu
Zn - Ni	*K* - Zn

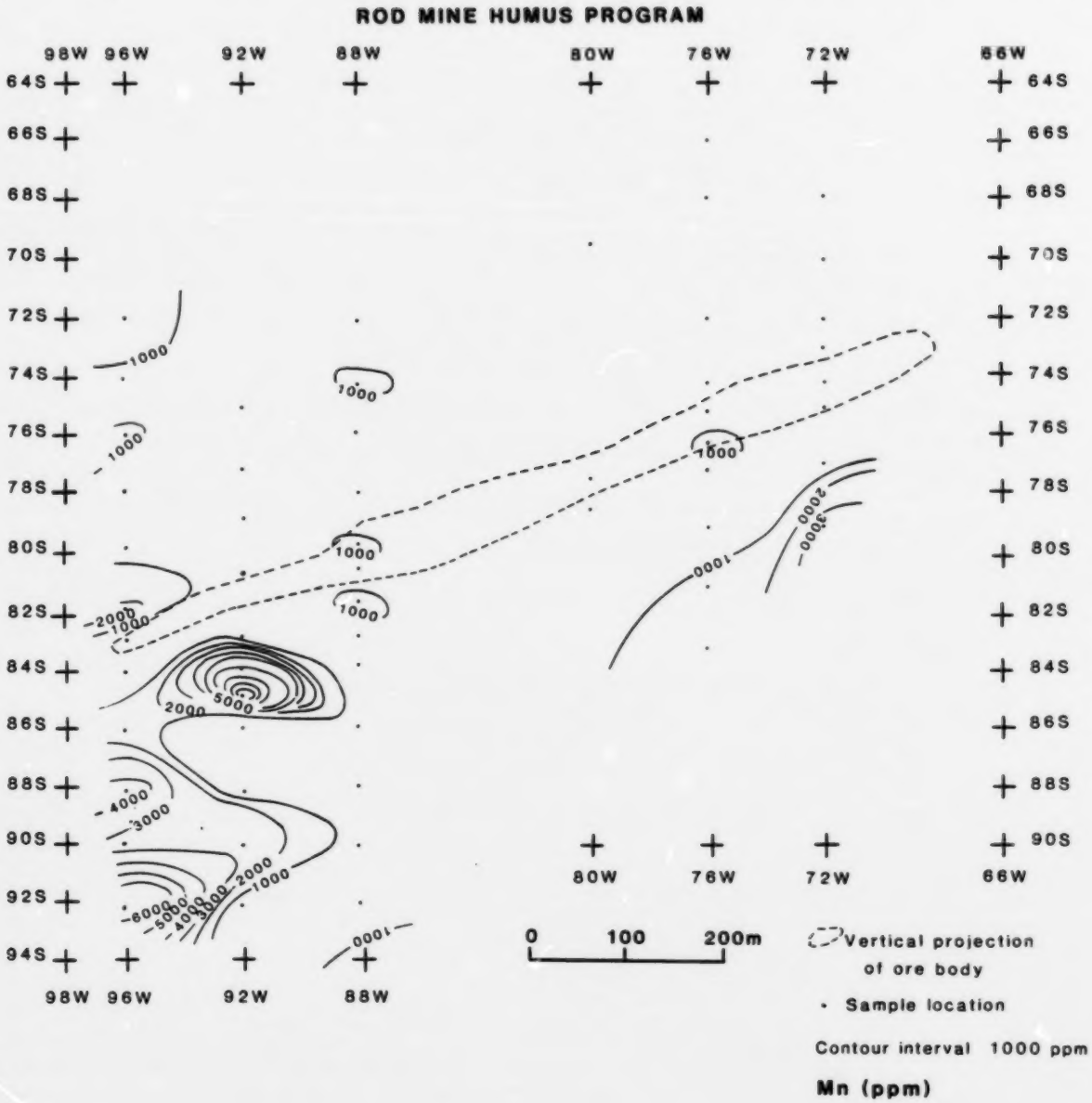

Figure 5: Contour diagram of Mn concentration in humus samples.

Manganese (Fig. 5)

Mn forms a 365 x 240 m anomaly with values up to 9044 ppm south of the vertical projection of the orebody at the western side of the sampled area. Other smaller anomalies occur just to the north of the largest anomaly (75 x 30 m) on the north side of the vertical projection (1000-2915 ppm) and at the southeastern edge of the sampled area (275 x 120 m; 1000-3016 ppm). Numerous single sample anomalies with values between 1000 and 2000 ppm occur throughout the sampled grid. Although these are greater than median and mode values which approximate 500 ppm, their limited extent and lower concentrations compared to the higher contrast anomalies diminish their importance.

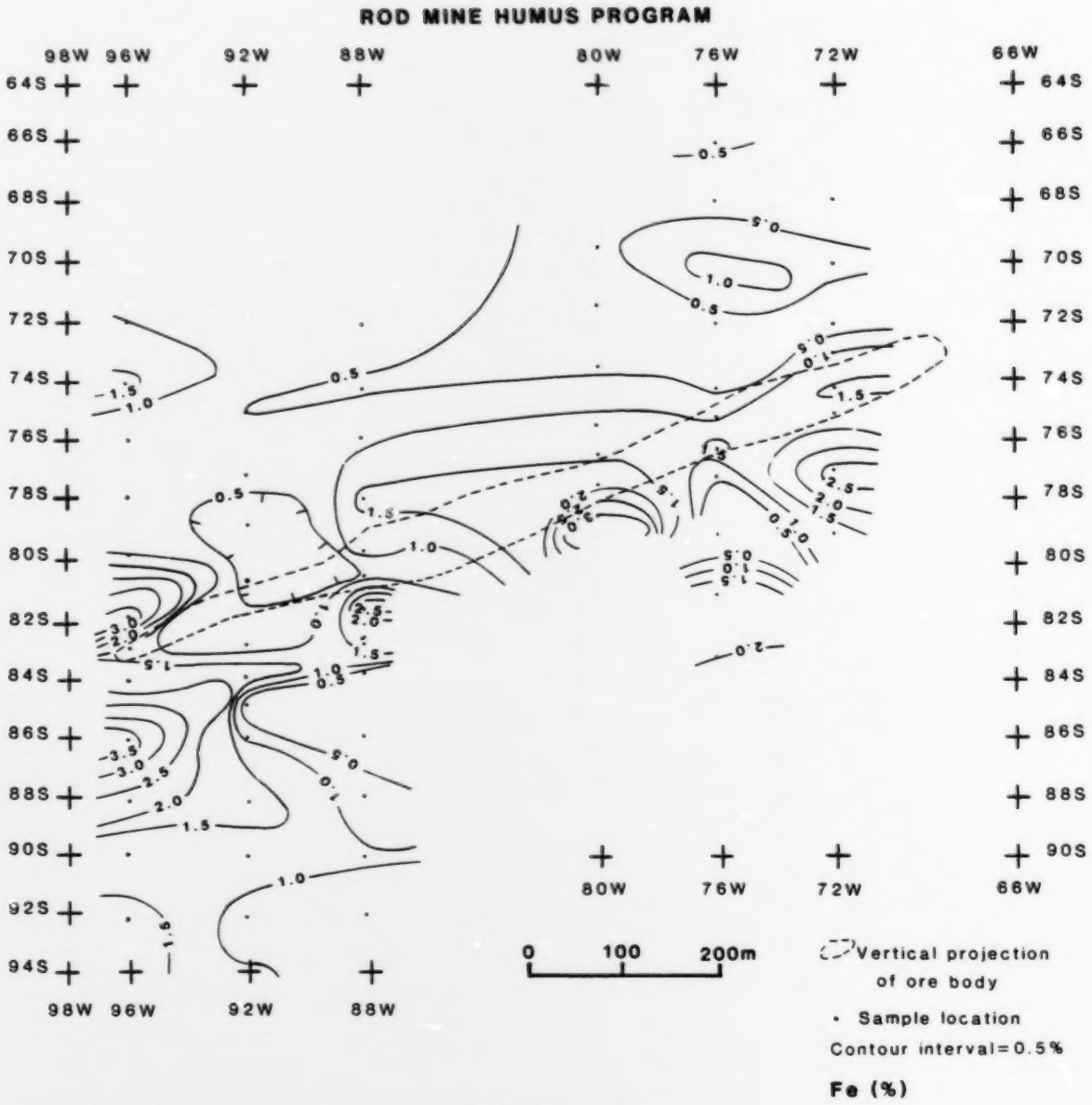
ROD MINE HUMUS PROGRAM
98W 96W 92W 88W 80W 76W 72W 66W
64S 66S 68S 70S 72S 74S 76S 78S 80S 82S 84S 86S 88S 90S 92S 94S
0 100 200m
Vertical projection of ore body
Sample location
Contour interval=0.5%
Fe (%)

Figure 6: Contour diagram of Fe concentration in humus samples.

Iron (Fig. 6)

Fe forms a low contrast broad anomaly (greater than 1.0%) over large parts of the southern part of the grid. Four anomalous areas ranging from 45 x 45 m to 150 x 120 m with values greater than 2.0% and up to 3.8% occur along the south flank of the vertical projection of the orebody and a fifth area (120 x 90 m; 1.0-3.2%) occurs on the north flank of the projection at the western edge of the study area. The two westernmost anomalies along line 96W are roughly coincident with Ni, Co, Zn, Cu and, to a lesser degree, Mn anomalies. The anomaly along line 88W coincides with the peak of the As anomaly. The anomalies along lines 80W and 72W do not appear to correlate with other variables. Small low contrast anomalies may be found at approximately L96W/74S (90 x 75 m; 1.0-1.5%) and L76W/70S (75 x 30 m; 1.0-1.3%); these are local and do not correlate with other element anomalies.

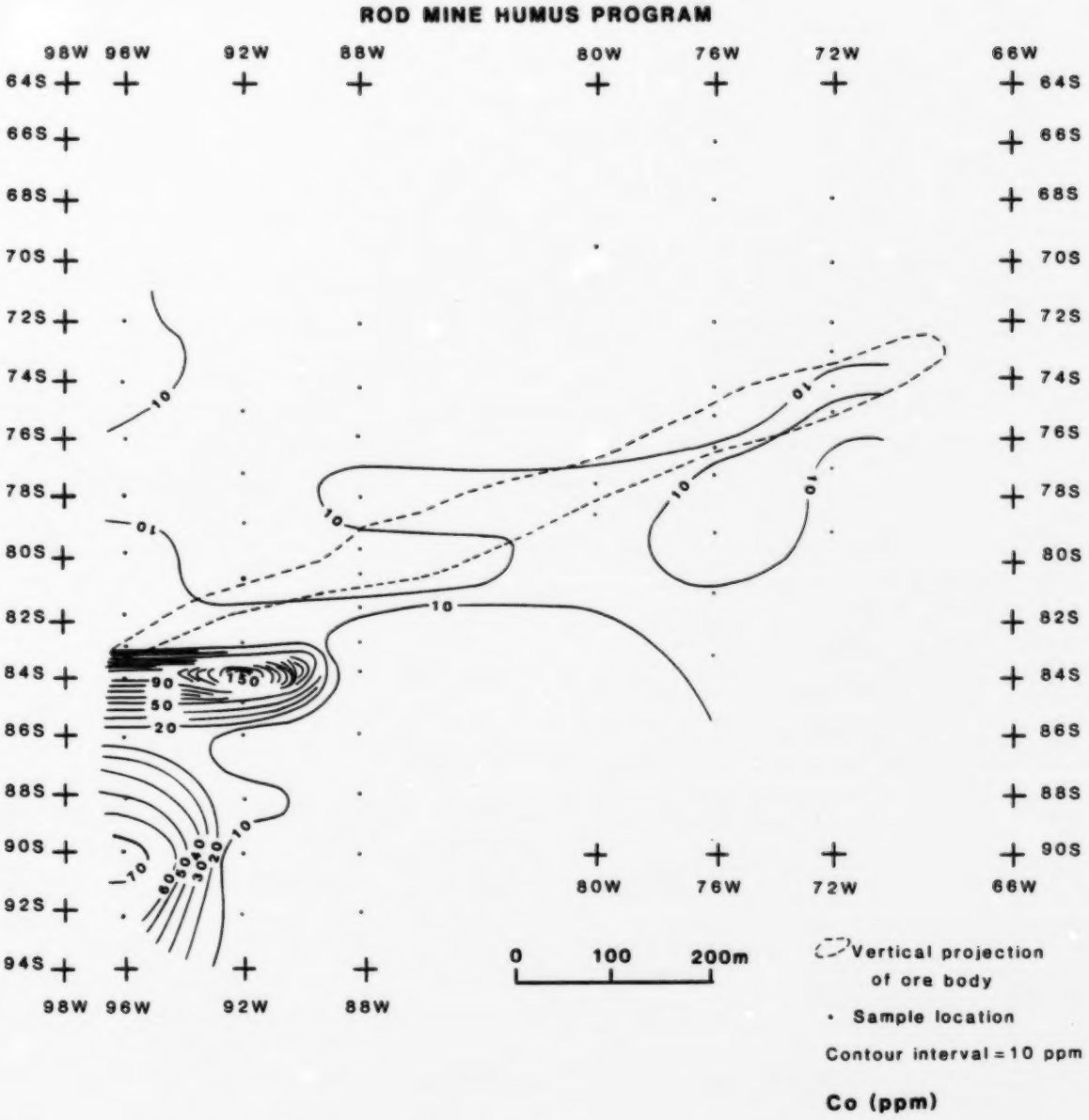

Figure 7: Contour diagram of Co concentration in humus samples.

Cobalt (Fig. 7)

Co forms marked anomalies in the southwestern part of the map area with anomalous values up to 166 ppm above a background of approximately 10 ppm. The anomalies occur as two distinct lobes along 84S from 98W to 90W and 86S-94S/98W-93W and together cover an area 365 x 240 m. These lobes have a strong correlation with similar anomalies in Zn, Cu, Ni, *K* and Mn.

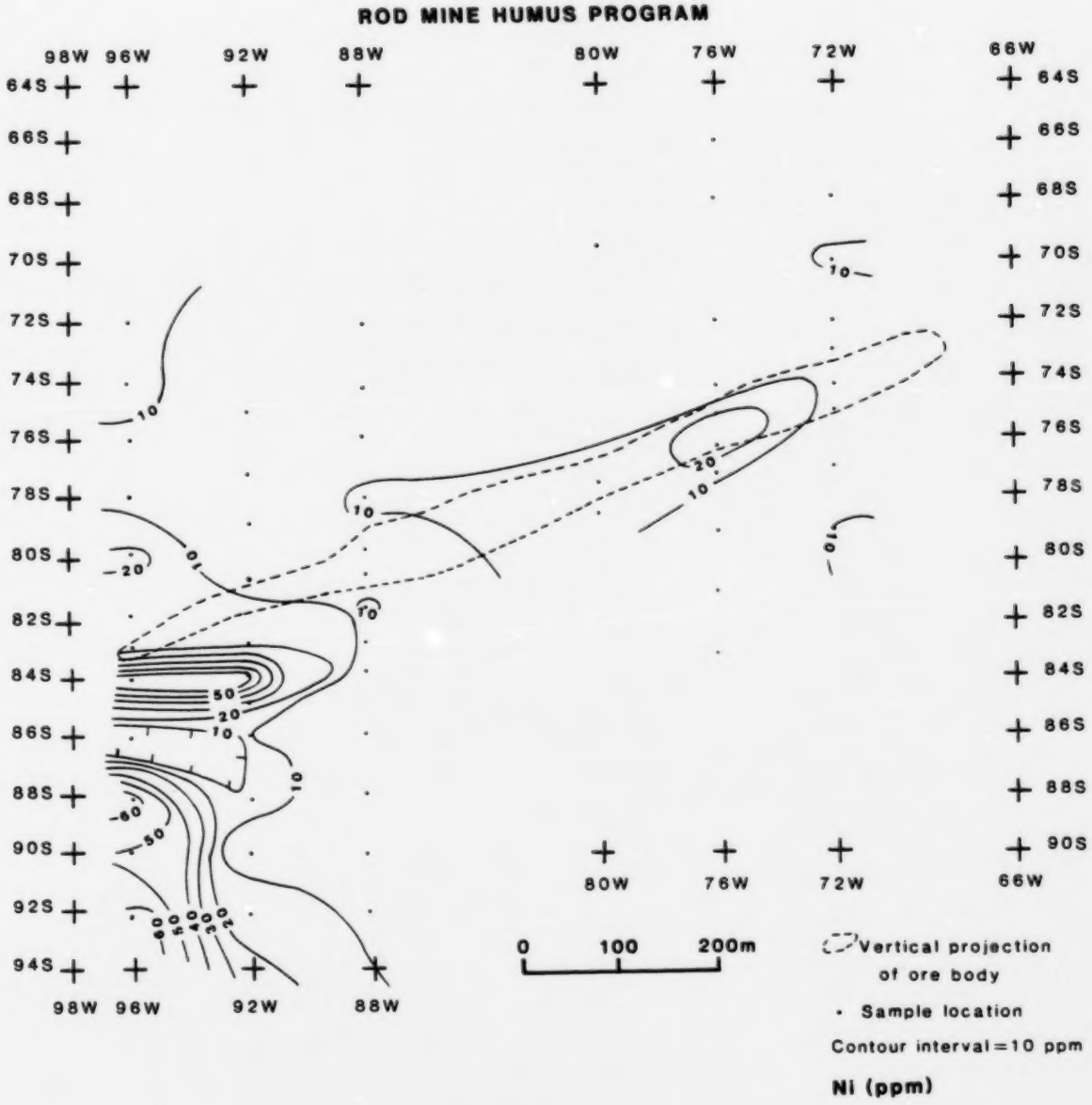
ROD MINE HUMUS PROGRAM
98W 96W 92W 88W 80W 76W 72W 66W
64S 66S 68S 70S 72S 74S 76S 78S 80S 82S 84S 86S 88S 90S 92S 94S
0 100 200m
Vertical projection of ore body
Sample location
Contour interval=10 ppm
Ni (ppm)

Figure 8: Contour diagram of Ni concentration in humus samples.

Nickel (Fig. 8)

Nickel forms two high contrast lobate anomalies together occupying an area 365 x 240 m with values greater than 20 ppm and up to 66 ppm in the southwestern part of the grid area coincident with anomalies for Co, Cu, Zn, *K*, and Mn. Two other localized low contrast anomalies occur at L96W/80S (30 x 30 m; 20-21 ppm), and at L76W/75-76S (105 x 45 m; 20-26 ppm).

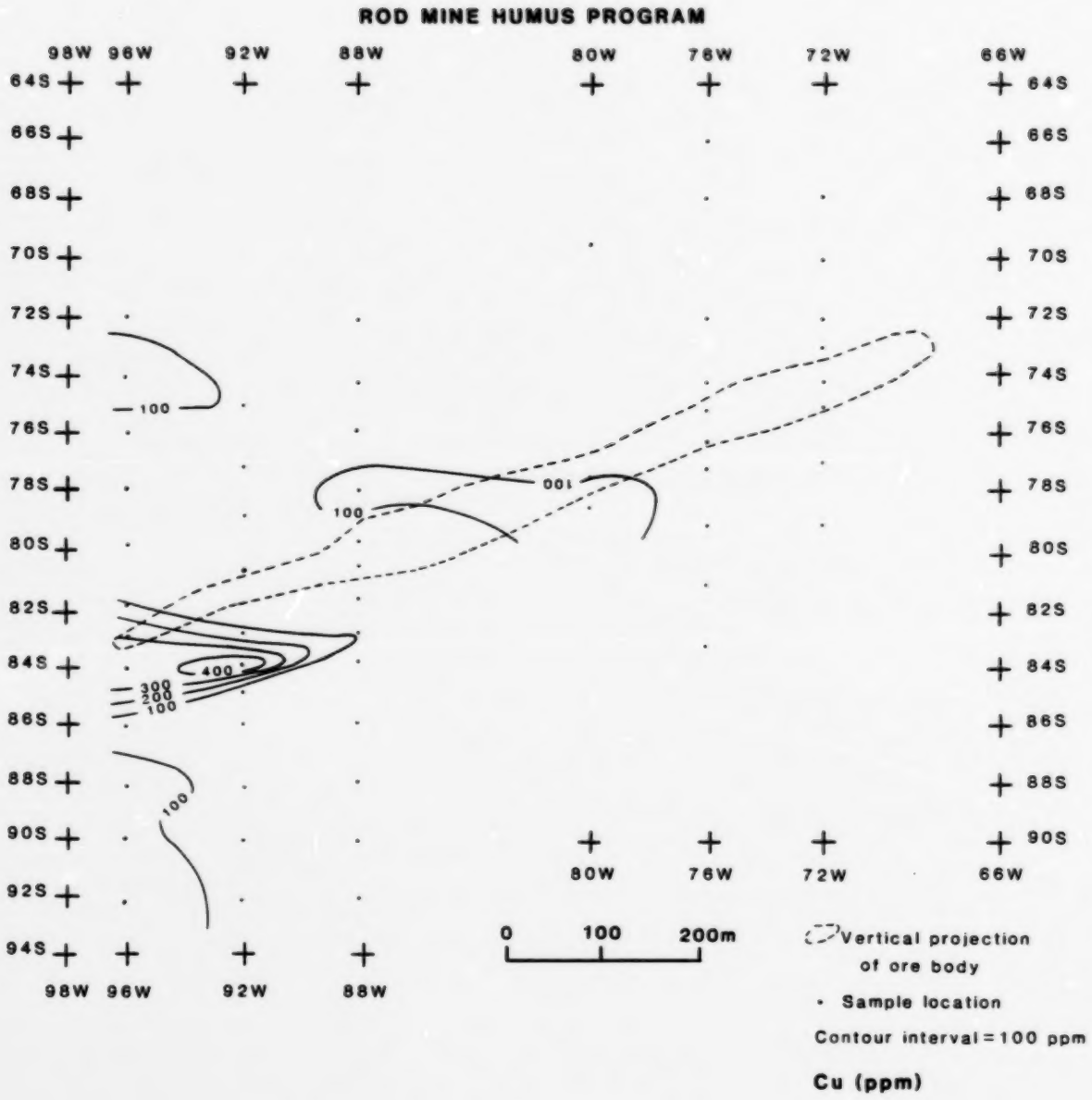

Figure 9: Contour diagram of Cu concentration in humus samples.

Copper (Fig. 9)

Copper forms a 260 x 90 m high contrast anomaly with a maximum concentration of 487 ppm along 84S/98W-89W that is coincident with anomalies for Co, Ni, Zn, *K* and Mn. Lesser anomalies with values greater than 100 ppm occur 1) along L96W from 87S to the southern limits of the grid area (180 x 60 m; up to 155 ppm), coincident with anomalies in Co, Ni, Zn, *K* and Mn; 2) near L96W/74S (105 x 75 m; up to 176 ppm) correlative with a Pb and a minor Zn anomaly; and 3) in the vicinity of 78S/90W-78W (100-157 ppm; 350 x 45 m), apparently not correlative with other element anomalies.

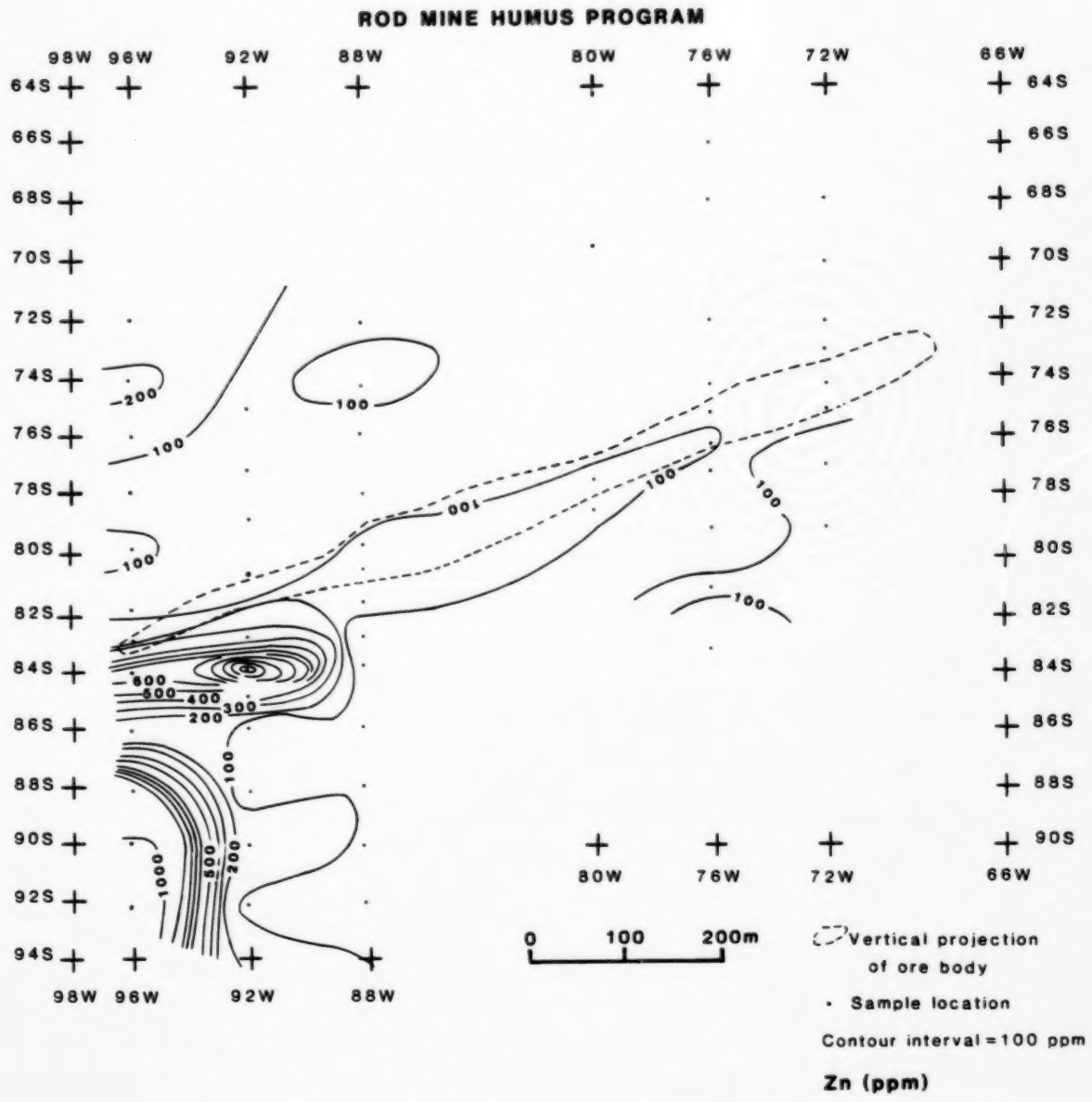

Figure 10: Contour diagram of Zn concentration in humus samples.

Zinc (Fig. 10)

Zinc forms two high contrast anomalies with greater than 100 ppm Zn totalling 365 x 240 m in the southwestern part of the sampled grid: 1) up to 1118 ppm in the area of 84S/98W-89W, and 2) up to 1236 ppm in the area of 96-93W/87-94S. These two lobes are coincident with anomalies in Cu, Co, Ni, *K* and Mn. A 180 x 120 m anomaly containing 100 to 214 ppm Zn occurs at the northwestern part of the grid area (approximately 72S-76S/98W-92W), coincident with a low contrast Cu anomaly.

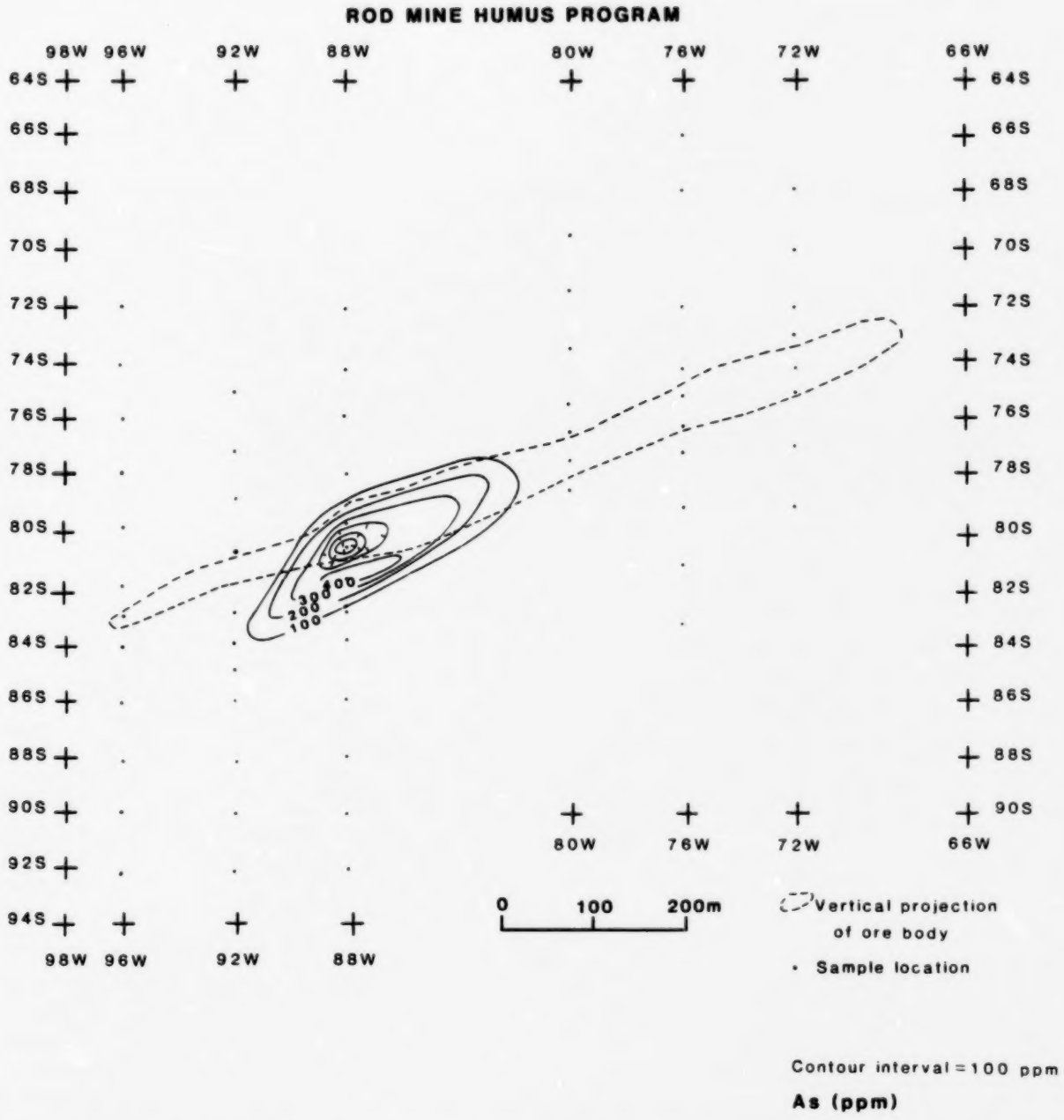
ROD MINE HUMUS PROGRAM
98W 96W 92W 88W 80W 76W 72W 66W
64S 66S 68S 70S 72S 74S 76S 78S 80S 82S 84S 86S 88S 90S 92S 94S
300
200
100
0 100 200m
Vertical projection of ore body
Sample location
Contour interval = 100 ppm
As (ppm)

Figure 11: Contour diagram of As concentration in humus samples.

Arsenic (Fig. 11)

Only nine analyses (representing eight sample sites including one duplicate pair of samples) contain As concentrations above the analytical lower limit of detection (5 ppm). A single oval-shaped anomaly (335 x 100 m) marked by values from 98 to 434 ppm is centred on L88W/82S. This anomaly, which corresponds to an Fe anomaly (2.0-2.6%), may correspond to the presence of Au-As mineralization noted in trenches apparently unrelated to the Rod ore zone (G. Kitzler, pers. comm.). Measurable concentrations of As are located also along L88W/72S-76S (14-39 ppm) and at L80W/69S (13 ppm).

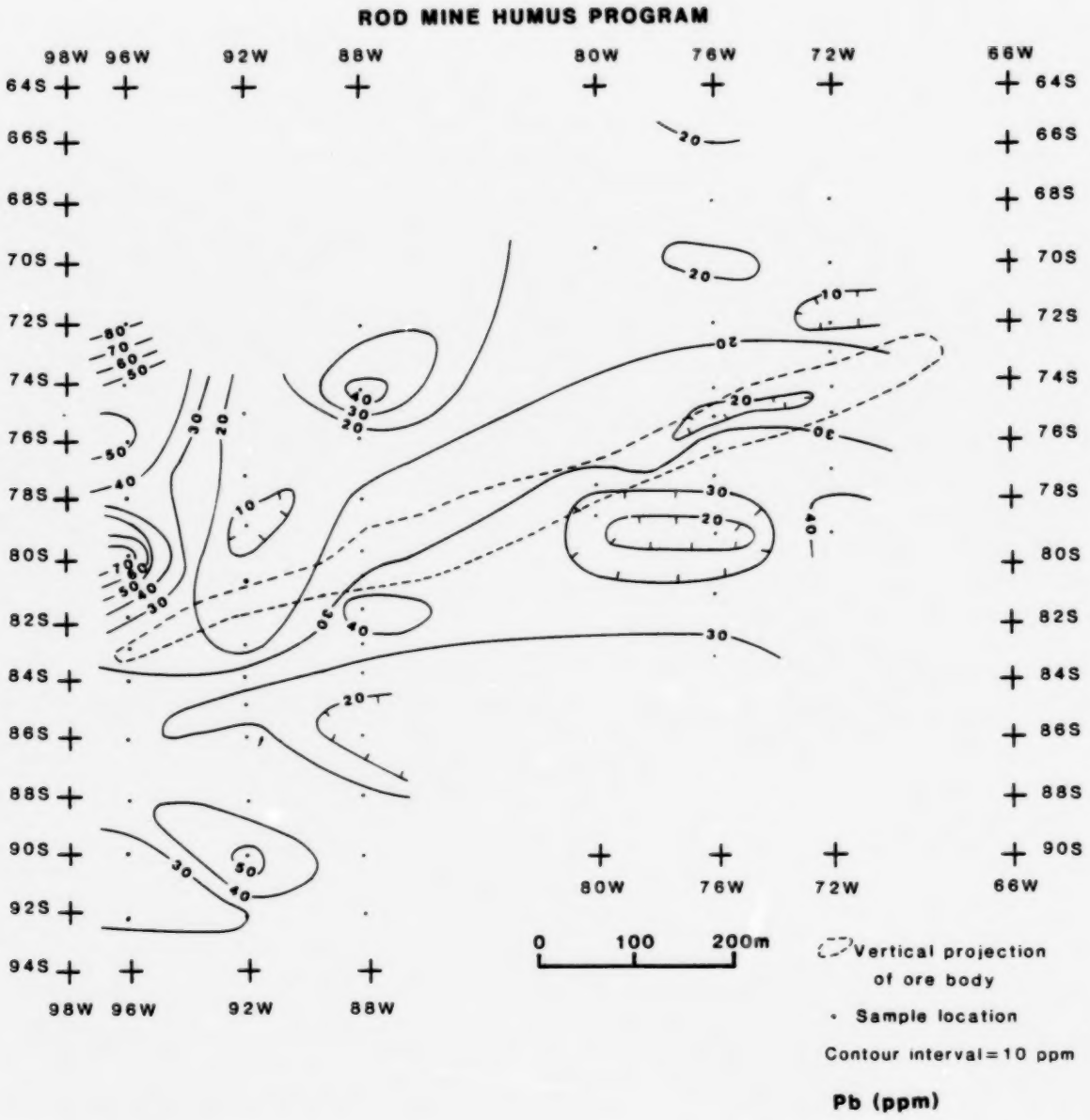
ROD MINE HUMUS PROGRAM
98W 96W 92W 88W 80W 76W 72W 66W
64S 66S 68S 70S 72S 74S 76S 78S 80S 82S 84S 86S 88S 90S 92S 94S
0 100 200m
Vertical projection of ore body
Sample location
Contour interval=10 ppm
Pb (ppm)

Figure 12: Contour diagram of Pb concentration in humus samples.

Lead (Fig. 12)

A 310 x 75 m Pb anomaly (30-81 ppm) occurs along L96W from 82S to the northern limit of the sampled grid. This anomaly corresponds with lower contrast, more localized Cu and Zn anomalies in this area. Other local anomalies are centred upon: 1) L92W/90S, 180 x 65 m (40-53 ppm); 2) L88W/82S, 90 x 45 m (40-49 ppm); 3) L88W/north of 75S, 190 x 120 m (30-42 ppm); and 4) L72W/79S, 60 x 60 m (40-44 ppm). The locations of Pb anomalies do not correlate well with those of other elements.

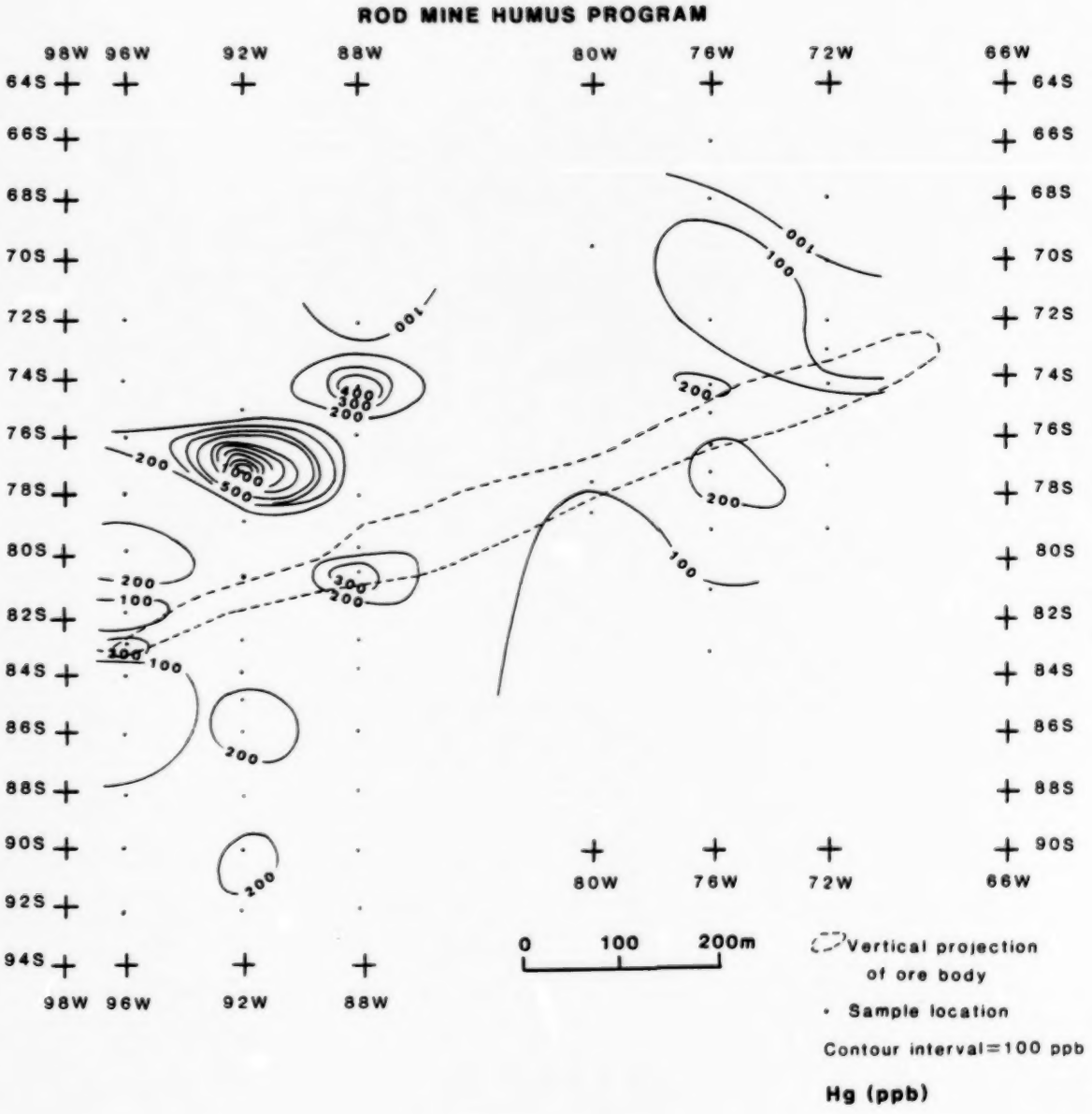

Figure 13: Contour diagram of Hg concentration in humus samples.

Mercury (Fig. 13)

Hg forms three localized anomalies: 1) at L92W/77S, 245 x 90 m (200-1110 ppm), 2) at L88W/74S, 135 x 60 m (200-420 ppm); and at L88W/82S, 110 x 40 m (200-340 ppm). Numerous local areas have values between 200 and 300 ppm. A visual correlation between the amount of Hg and values for other elements is not apparent.

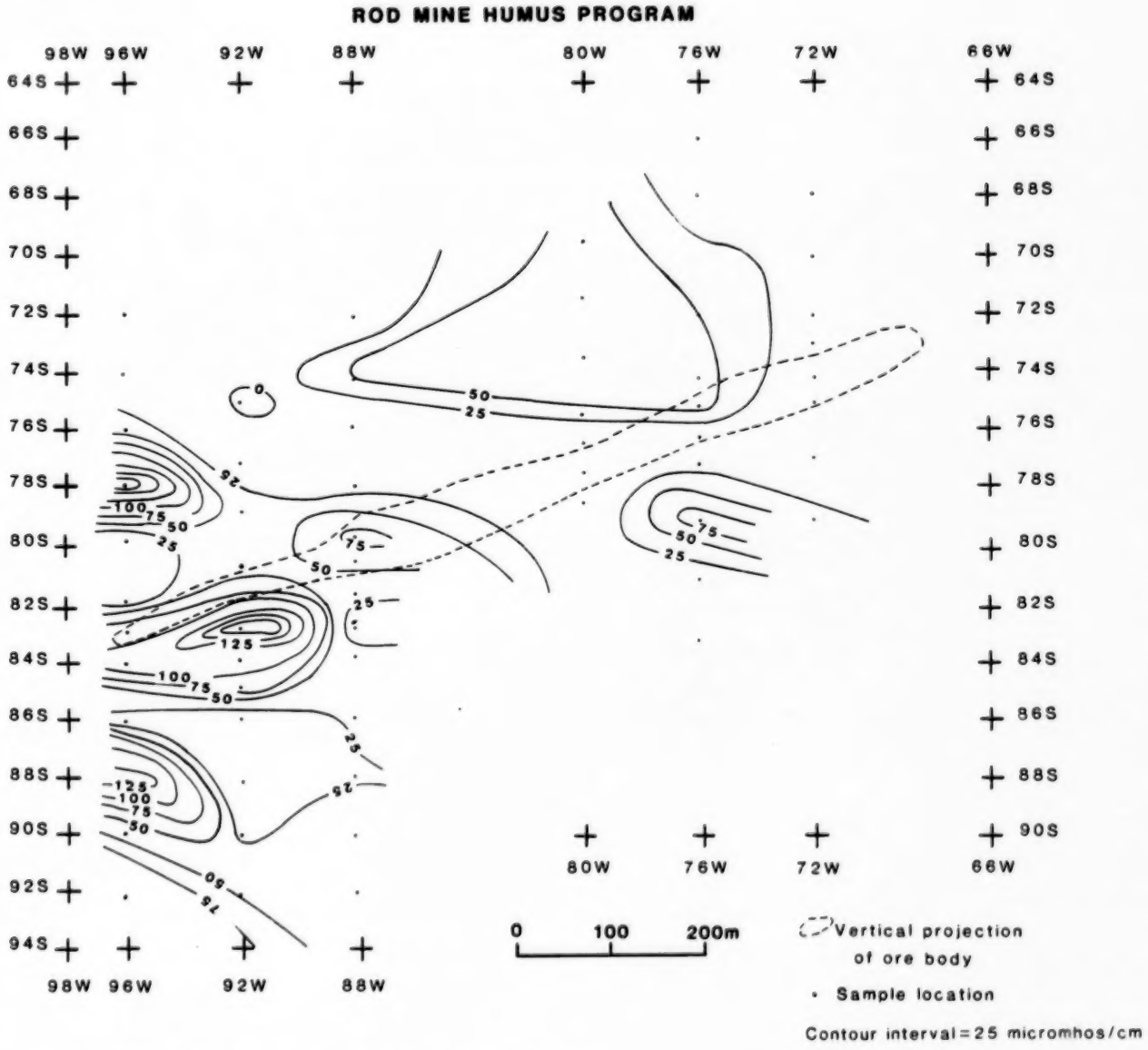
ROD MINE HUMUS PROGRAM
98W 96W 92W 88W 80W 76W 72W 66W
64S 66S 68S 70S 72S 74S 76S 78S 80S 82S 84S 86S 88S 90S 92S 94S
0 100 200m
Vertical projection of ore body
Sample location
Contour interval=25 micromhos/cm
K (micromhos/cm)

Figure 14: Contour diagram of *K* variation in humus samples.

Specific conductance (*K*) (Fig. 14)

Conductivity readings were converted to units of specific conductance by multiplying by the cell constant and were corrected for H^+ concentration by the formula derived by Govett (1976):

$K = (k_s - k_{H2O}) - 0.34982(H_s^+ - H_{H2O}^+)$ $ohms^{-1}cm^{-1}$

where K = specific conductance corrected for H^+ concentration; k_s = specific conductance of soil slurry; k_{H2O} = specific conductance of water; H_s^+ = hydrogen ion concentration of soil slurry; H_{H2O}^+ = hydrogen ion concentration of water.

A contour of specific conductance reveals the location of three anomalies along the western part of the grid map. These are 1) in the vicinity of 84S/98W-89W (245 x 120 m; 50-183 micromhos/cm); 2) centred on L96W/88S (120 x 90 m; 50-134 micromhos/cm); and 3) centred around L96W/78S (120 x 90 m; 50-180 micromhos/cm). The first two anomalies coincide with Co, Ni, Cu, Zn and Mn anomalies. The third anomaly

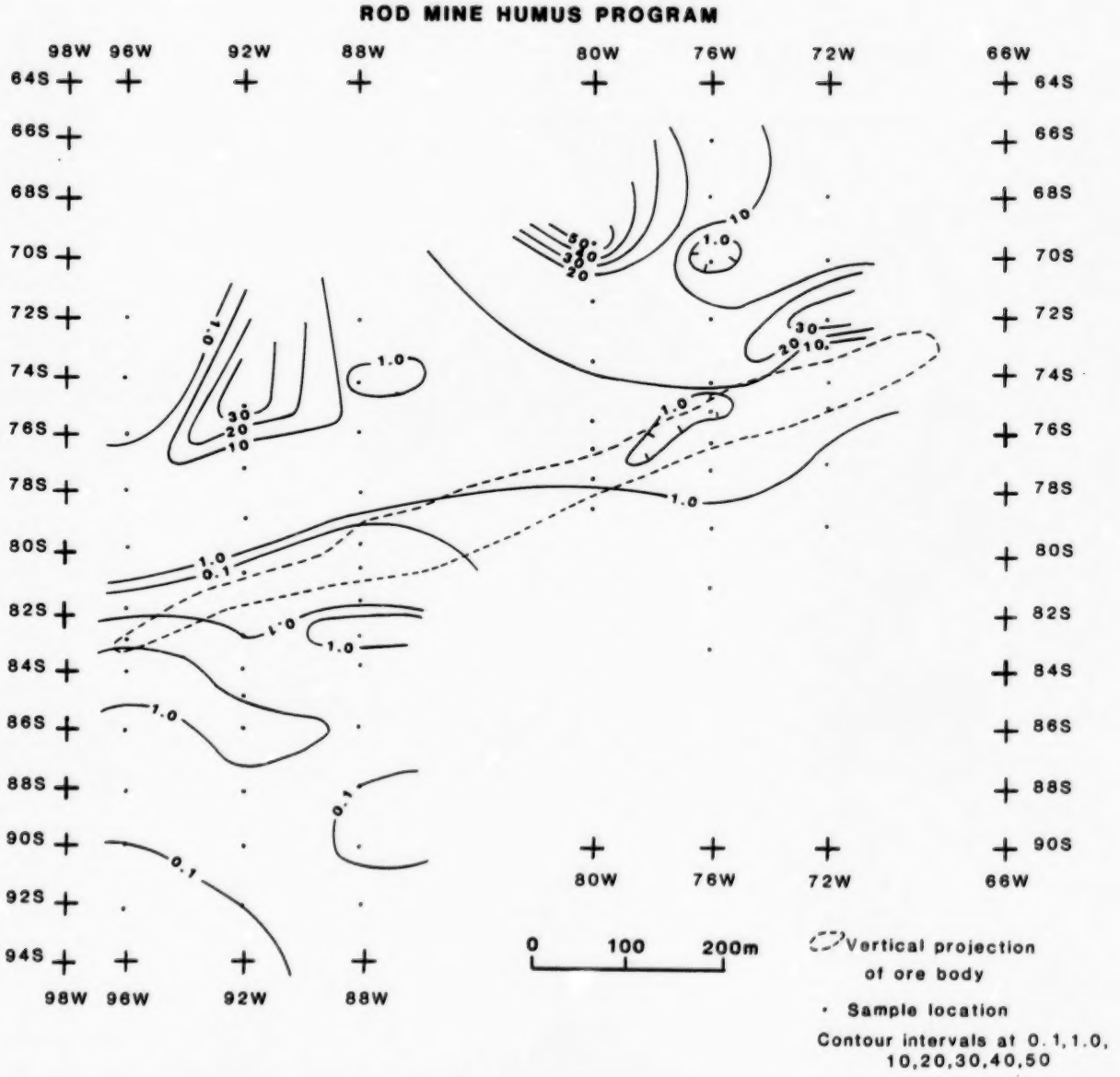
ROD MINE HUMUS PROGRAM
98W 96W 92W 88W 80W 76W 72W 66W
64S 66S 68S 70S 72S 74S 76S 78S 80S 82S 84S 86S 88S 90S 92S 94S
0 100 200m
Vertical projection of ore body
Sample location
Contour intervals at 0.1, 1.0, 10, 20, 30, 40, 50
H+ (ppm)

Figure 15: Contour diagram of H^+ concentration in humus samples.

may represent part of this same general anomalous area because of its close proximity.

Hydrogen ion (Fig. 15)

The plot of H^+ values is more amenable to contouring at irregularly defined intervals, i.e. at 0.1, 1.0, 10, 20, 30, 40, 50 ppm. Govett (1976) declined to use pH as the mode of presentation stating that plots of H^+ are more sensitive and highlight differences in H^+ concentration better than the logarithmic equivalent, pH. This logic is applied here for similar reasons and to allow for ease of comparison of results between this study and Govett's (1976) case study. Anomalously high concentrations of H^+ (greater than 1.0 ppm) occur at: 1) L92W/75S (150 x 120 m; 37 ppm), 2) L80W/69S (150 x 60 m; 55 ppm), and 3) L72W/72S (150 x 60 m; 33 ppm). These do not appear to correlate with other analyzed elemental abundances. Anomalously low concentrations

of H^+ are found: 1) in a 365 x 75 m band along 82S/98W-84W (0.1-0.03 ppm), 2) at L88W/88-90S (90 x 90 m; 0.1-0.05 ppm), and 3) in a 240 x 75 m band along the southwestern corner of the map area at approximately 92W-98W/90S-94S (0.1-0.06 ppm). Although these do not appear to have a direct correlation with other elements, the anomalous low areas roughly abut the high coincident anomaly of Co, Ni, Zn and Cu.

Summary

A consistent multi-element geochemical anomaly for Cu, Zn, Co, Ni, Fe and Mn is noted in the southwestern part of the grid. It occurs slightly over and to the south of the vertical projection of the Rod deposit. This 365 x 240 m anomaly has two distinctive lobes: 1) along 84S from 98W to 90W, and 2) 86S-94S/98W-93W. Specific conductance (*K*) values duplicate the location and range in concentration of this anomaly.

The hydrogen ion concentration (H^+) forms a very weak positive anomaly coincident with the previously discussed multi-element anomaly. The significance of this is uncertain, especially in light of the magnitude of H^+ anomalies at the northern end of the sampling area.

The As values delineate an area with known near-surface Au mineralization, (mobilizate?) unrelated to the Rod Cu-Zn deposit. Fe values also correspond to the As anomaly, partly coincide with the previously described multi-element anomaly, and yield some anomalies of uncertain origin.

Hg anomalies are of uncertain origin, but they could possibly reflect variations in the Hg content of the mineralized zone. No relationship is observed between the Hg content of the humus and the results of a Hg-gas survey conducted over the Rod deposit by Fedikow (1986a). Maciolek and Jones (1987) noted that the various modes of occurrence of Hg have different capabilities for dispersion away from the source of the Hg. Thus, the different patterns of Hg concentration found for the humus and Hg-gas surveys may be a reflection of a difference of Hg forms.

Pb anomalies are, for the most part, unrelated to multiple anomalies observed for the rest of the elements in this survey.

DISCUSSION

The analysis of metal concentrations in humus samples is widely used as an exploration tool in the search for sulphide deposits (Brooks, 1983). Anomalies may occur in nonmineralized rocks or glacial overburden overlying sulphide deposits as the result of electrochemical dispersion as well as the simpler mechanism of meteoric water transport (Govett, 1973; Nuutilainen and Peuraniemi, 1977; Govett, 1976). There is a general decrease in Eh with increasing depth in the earth's crust. The presence of an electron conductor, such as a sulphide or graphite deposit, causes a disruption in the distribution of oxidation potentials. The differences in Eh along the margins of the sulphide body lead to the generation of natural galvanic forces that could be confirmed by a self potential survey. Thus, a redox cell in which the uppermost part of a sulphide deposit acts as a cathode and the lowermost part acts as an anode, is created leading to a net upward motion of hydrogen ions and other cations, and a net downward motion of hydroxyl ions and other anions (Govett, 1976). The result would be an anomalous concentration of H^+ and other cations, measurable by pH and conductivity tests, over a sulphide deposit. In support of his model, Govett (1976) showed in a case study over the White Lake Zn-Cu mine near Flin Flon that his approach yielded results that correlated with other trace element anomalies in humus and with the location of the White Lake deposit.

In this study conductivity anomalies, measured as specific conductance, *K*, appear to be reasonable indicators of anomalous sulphide element (Zn, Cu, Co, Ni, Mn, Fe) concentrations (see Results). The role of the hydrogen ion is less obvious here (see Results). Govett (1976) stresses that the shape or relative magnitude of an anomaly among adjacent samples is more important than absolute numerical magnitudes. This reasoning could possibly justify correlating the multi-element and *K* anomaly in the southwestern part of the grid with a modest H^+ anomaly flanked by anomalously low values. However, large H^+ values along the northern part of the area remain unexplained, and possible buffering effects by the widespread carbonate alteration cannot be ignored.

The position of the *K* and multi-element anomaly in the southwestern area of the grid is slightly south of the vertical projection of the western uppermost part of the orebody in the updip direction. The southwestern end of the ore zone is buried beneath 1 - 6 m of overburden and 183 m of bedrock. The more deeply buried (732 m) northeastern end of the deposit did not elicit an anomalous response. Local Fe, Mn, Co and Pb anomalies occur southeast of the deeper end of the body, but it is doubtful that these smaller, more localized, lower contrast anomalies occur in response to Cu-Zn mineralization at extreme depth. Drainage patterns with particular concern to Stall Lake and the nearby Stall Lake mine should be verified before the multi-element anomaly is considered or rejected as attributable to dispersion of elements from the Rod deposit. If the multi-element anomaly can be determined to be uninfluenced by drainage from a source of metals separate from the Rod mine, then the difference in trace metal response between the western and eastern ends of the ore zone implies a depth of burial exists below which humus geochemical analysis is ineffective.

These results suggest that for humus geochemical surveys the measurement of specific conductance and perhaps H^+ may be used as a pre-screening tool to reduce large areas of potential interest to more localized areas where more expensive exploration techniques can be focussed. Measurement of *K* and H^+ is rapid, simple, inexpensive and nondestructive in comparison to standard laboratory analytical techniques for measuring trace metal contents.

Future Work and Recommendations

The size of the sampled area for this study was chosen to cover the extent of the No. 2 Zone. Future work is planned to extend coverage of the survey area to encompass the nearby near surface No. 1 Zone and surrounding area in an attempt to put the anomalies outlined in this study into a more regional areal perspective, and to further test *K* and H^+ response and their correlation to trace element anomalies over a larger area with shallower mineralization.

Govett (1976) noted the importance of close sample spacings in studies of this nature; in the White Lake study spacings of 25 ft. reduced to 10 ft. over the deposit were used. The 61 m and 30.5 m spacings used here seem adequate, but spacings probably should be no greater than those used here.

CONCLUSIONS

The following conclusions are drawn from the results of this study:

(1) A consistent multi-element humus geochemical anomaly was generated over the southwestern end of the Rod Cu-Zn deposit, No. 2 Zone. Cu, Zn, Co, Ni, Fe and Mn yield coincident anomalies in this area. (2) Specific conductance (*K*) values are correlative with results for the more routine trace element analyses. (3) *K*, and perhaps H^+, measurements may be useful as a potential exploration technique to prescreen large areas of interest in an effort to locate smaller anomalous areas on which to focus more intensive, more expensive exploration techniques. (4) No relationship is observed between the Hg content of the humus samples and the results of a Hg-gas survey conducted over the Rod deposit.

Acknowledgments

The authors wish to acknowledge the cooperation of T. Baumgartner and G. Kitzler from Hudson Bay Exploration & Development Co. Ltd. and D. Ziehlke of Snow Lake Mines Ltd., and to thank them for information and valuable discussions. C. Roney collected the humus samples. Analytical assistance provided by J. Gregorchuk is appreciated. G. Gale, D. McRitchie and B. Bannatyne provided constructive criticism and editorial review. S. Weselak typed the manuscript.

REFERENCES

Balles, A.H., Syme, E.C., Galley, A., Price, D.P., Skirrow, R. and Ziehlke, D.J.
1987: Early Proterozoic volcanism, hydrothermal activity, and associated ore deposits at Flin Flon and Snow Lake, Manitoba; Geological Association of Canada Field Trip Guidebook 1987 Trip 1, 95 p.

Brooks, R.
1983: Biological Methods of Prospecting for Minerals; John Wiley & Sons, Toronto.

Bruce, E.L.
1918: Amisk-Athapapuskow Lake district; Geological Survey of Canada, Memoir 105.

Coats, C.J.A., Clark, L.A., Buchan, R. and Brummer, J.J.
1970: Geology of the copper-zinc deposits of Stall Lake Mines Ltd., Snow Lake area, N. Manitoba; Economic Geology, v. 65, p. 970-984.

Esposito, B.
1986: Copper and zinc in Manitoba; Manitoba Energy and Mines, Mineral Education Series, 24. p.

Fedikow, M.A.F.
1986a: Mercury gas surveys over base and precious metal mineral deposits in the Lynn Lake and Snow Lake areas, Manitoba; Manitoba Energy and Mines, Open File Report OF85-11.

Fedikow, M.A.F.
1986b: Detection of gold mineralization and lithologic mapping within the Agassiz Metallotect (Lynn Lake area) utilizing black spruce *(Picea mariana)* bark; Manitoba Energy and Mines, Open File Report OF86-6.

Fedikow, M.A.F. and Ferreira, K.J.
1987: Results of a rock geochemical survey of the Lynn Lake Rhyolitic Complex; Manitoba Energy and Mines, Open File Report OF87-6.

Froese, E. and Moore, J.M.
1980: Metamorphism in the Snow Lake area, Manitoba; Geological Survey of Canada, Paper 78-27.

Govett, G.J.S.
1973: Differential secondary dispersion in transported soils and post-mineralization rocks: an electrochemical interpretation; in M.J. Jones (ed.), Geochemical Exploration 1972, Institute of Mining and Metallurgy, London, p. 81-91.

Govett, G.J.S.
1976: Detection of deeply buried and blind sulphide deposits by measurement of H^+ and conductivity of closely spaced surface soil samples; Journal of Geochemical Exploration, v. 6, p. 359-382.

Maciolek, J.B. and Jones, V.T.
1987: Mobile mercury application in the search for gold; Explore: the Association of Exploration Geochemists Newsletter, No. 61, October 1987, p. 6-7.

Nuutilainen, J. and Peuraniemi, V.
1977: Application of humus analysis to geochemical prospecting: some case histories; in Prospecting in Areas of Glaciated Terrain, Institution of Mining and Metallurgy, London.

Tennant, C.B. and White, M.L.
1959: Studies of the distribution of some geochemical data; Economic Geology, v. 54, p. 1281-1291.

APPENDIX I

RESULTS OF ANALYZING DIFFERENT SIZE FRACTIONS FOR REPRESENTATIVE SAMPLES OF HUMUS

Sample Number	Mn ppm	Fe %	Co ppm	Ni ppm	Cu ppm	Zn ppm	Mo ppm	Ag ppm	Pb ppm	As ppm
Less than 2 micron size fraction										
1793	*	*	*	*	*	*	*	*	*	2
1794	400	0.6	4	5	95	44	<1	<0.1	16	3
1795	*	*	*	*	*	*	*	*	*	*
1796	*	*	*	*	*	*	*	*	*	*
-80 mesh size fraction										
1793	720	0.8	9	5	29	35	<1	<0.1	8	2
1794	2400	0.4	5	5	34	90	1	<0.1	8	4
1795	1100	0.4	2	3	21	83	<1	<0.1	14	3
1796	440	0.8	3	4	58	32	<1	<0.1	8	124

*-Insufficient sample

APPENDIX II

ANALYTICAL SPECIFICATIONS

Element	Size Fraction	Sample Weight	Method of Extraction	Method	Lower Limit of Detection	Ashed
Manganese	-80	0.5 g	$HCl-HNO_3$ (1:3)	DCP	1 ppm	no
Iron	-80	0.5 g	$HCl-HNO_3$ (1:3)	DCP	0.1%	no
Cobalt	-80	0.5 g	$HCl-HNO_3$ (1:3)	DCP	1 ppm	no
Nickel	-80	0.5 g	$HCl-HNO_3$ (1:3)	DCP	1 ppm	no
Copper	-80	0.5 g	$HCl-HNO_3$ (1:3)	DCP	1 ppm	no
Zinc	-80	0.5 g	$HCl-HNO_3$ (1:3)	DCP	1 ppm	no
Arsenic	-80	0.5 g	$HCl-HNO_3$ (1:3)	DCP	5 ppm	no
Molybdenum	-80	0.5 g	$HCl-HNO_3$ (1:3)	DCP	1 ppm	no
Silver	-80	0.5 g	$HCl-HNO_3$ (1:3)	DCP	0.5 ppm	no
Antimony	-80	0.5 g	$HCl-HNO_3$ (1:3)	DCP	5 ppm	no
Lead	-80	0.5 g	$HCl-HNO_3$ (1:3)	DCP	5 ppm	no
Bismuth	-80	0.5 g	$HCl-HNO_3$ (1:3)	DCP	2 ppm	no
Mercury	-80	0.5 g	$HNO_3-H_2SO_4-HCl-KMnO_4$	Cold Vapour AA	5 ppb	no

Determination of Conductivity and pH:

A 0.500 g standardized sample is suspended as a slurry in 100 ml deionized water. Conductivity and pH are measured with the following instrumentation:

Conductivity: "Radiometer" Conductivity Meter. Type CDM2e
"Radiometer" Conductivity Electrode. Type CDC 104.

pH: "Fisher Accumet" pH Meter. Model 620.
"Fisher" Universal Glass pH Electrode. #13-639-3.
"Fisher" Calomel Reference Electrode. #13-639-62.

APPENDIX III

RAW DATA

Sample Number	Mn ppm	Fe %	Co ppm	Ni ppm	Cu ppm	Zn ppm	As ppm	Mo ppm	Ag ppm	Sb ppm	Pb ppm	Bi ppm	Hg ppb	*K* micro-mhos/cm	H^+ ppm
1751	1720	1.0	11	11	89	163	<5	2	<0.5	<5	81	<2	160	16	0.32
1752	703	1.5	15	11	176	214	<5	1	<0.5	<5	49	<2	135	15	0.23
1753	1084	0.5	8	9	54	111	<5	1	<0.5	<5	51	<2	205	28	0.40
1754	565	0.9	3	5	34	37	<5	2	<0.5	<5	35	<2	100	180	8.3
1755	821	1.0	14	21	75	100	<5	2	<0.5	<5	77	<2	290	19	9.1
1756	2914	3.2	16	13	101	73	<5	3	<0.5	<5	33	<2	85	24	0.03
1757	209	1.2	11	15	285	166	<5	3	<0.5	<5	22	<2	210	84	0.19
1758	430	1.4	143	83	271	881	<5	2	<0.5	<5	35	<2	85	172	5.5
1759	312	2.0	53	48	417	328	<5	2	<0.5	<5	30	<2	90	56	1.1
1760	1426	3.8	17	6	63	165	<5	2	<0.5	<5	32	<2	55	20	0.81
1761	4041	2.3	50	61	140	987	<5	3	<0.5	<5	38	<2	125	134	0.21
1762	2768	1.1	73	46	125	1076	<5	2	<0.5	<5	24	<2	155	42	0.11
1763	6760	1.7	65	62	155	1236	<5	3	<0.5	<5	29	<2	125	98	0.06
1764	599	1.1	5	26	47	150	<5	3	<0.5	<5	35	<2	125	73	0.06
1765	947	0.8	4	14	64	50	<5	2	<0.5	<5	30	<2	190	49	0.10
1766	2571	1.3	7	7	28	179	<5	2	<0.5	<5	53	<2	215	22	0.48
1767	752	1.7	13	12	64	67	<5	2	<0.5	<5	36	<2	105	15	0.71
1768	396	0.9	6	10	31	87	<5	1	<0.5	<5	33	<2	230	14	2.8
1769	948	0.5	14	23	53	397	<5	2	<0.5	<5	18	<2	125	76	0.09
1770	17140	0.3	49	20	75	417	<5	3	<0.5	<5	32	<2	355	98	0.13
1771	6480	1.9	166	65	487	1118	98	1	<0.5	<5	35	<2	125	114	0.47
1772	437	0.6	17	20	109	364	<5	2	<0.5	<5	18	<2	145	183	0.10
1773	541	0.4	3	5	38	43	<5	2	<0.5	<5	14	<2	165	47	0.06
1774	30	<0.1	<1	<1	9	14	<5	2	<0.5	<5	6	<2	105	32	8.3
1775	250	0.8	5	4	24	45	<5	<1	<0.5	<5	17	<2	1110	12	6.0
1776	64	0.5	4	6	80	69	<5	2	<0.5	<5	6	<2	160	2	37.0
1777	1474	0.6	8	10	32	97	<5	<1	<0.5	<5	30	<2	175	17	0.49
1778	339	0.8	5	8	28	76	<5	1	<0.5	<5	34	<2	145	14	0.87
1779	610	1.1	6	9	42	87	<5	1	<0.5	<5	30	<2	140	35	0.05
1780	715	0.8	5	7	56	95	<5	1	<0.5	<5	35	<2	185	22	0.12
1781	65	0.2	<1	3	14	16	<5	2	<0.5	<5	15	<2	155	35	0.35
1782	136	0.4	2	4	30	40	<5	2	<0.5	<5	24	<2	125	28	0.60

RAW DATA (Cont'd.)

Sample Number	Mn ppm	Fe %	Co ppm	Ni ppm	Cu ppm	Zn ppm	As ppm	Mo ppm	Ag ppm	Sb ppm	Pb ppm	Bi ppm	Hg ppb	*K* micro-mhos/cm	H^+ ppm
1783	123	1.5	4	9	98	63	<5	1	<0.5	<5	36	<2	145	7	1.6
1784	1272	2.6	13	10	61	153	434	2	<0.5	<5	49	<2	185	38	0.50
1785	371	0.5	4	9	107	191	42	2	<0.5	<5	32	<2	375	39	0.72
1786	665	0.4	3	6	44	99	56	2	<0.5	<5	28	<2	305	68	0.63
1787	1098	1.2	6	7	52	121	378	3	<0.5	<5	28	<2	160	79	0.11
1788	751	1.6	17	12	146	42	<5	1	<0.5	<5	24	<2	120	24	1.1
1789	88	0.9	4	4	54	37	14	1	<0.5	<5	14	<2	100	6	4.7
1790	1154	0.4	2	8	100	196	39	1	0.5	<5	42	<2	420	50	0.89
1791	158	0.9	6	7	54	59	14	1	0.7	<5	25	<2	85	13	3.5
1792	120	0.3	3	4	28	41	13	3	<0.5	<5	17	<2	165	63	55.0
1797	823	1.5	10	13	100	75	<5	1	<0.5	<5	32	<2	115	19	1.3
1798	789	1.9	14	14	96	129	<5	2	<0.5	<5	38	<2	105	12	0.89
1799	263	3.0	18	14	157	109	<5	2	<0.5	<5	22	<2	60	16	0.68
1800	55	0.6	2	6	41	35	<5	2	<0.5	<5	20	<2	50	6	13.0
1801	83	0.3	3	6	57	44	<5	2	<0.5	<5	17	<2	105	6	17.0
1802	210	1.3	5	8	40	67	<5	1	<0.5	<5	22	<2	50	32	0.54
1803	37	0.4	2	5	36	53	<5	3	<0.5	<5	14	<2	40	60	12.0
1804	44	0.4	2	6	25	33	<5	2	<0.5	<5	17	<2	20	39	9.3
1805	437	0.4	1	5	21	90	<5	2	<0.5	<5	27	<2	240	52	14.0
1806	589	0.9	5	20	57	46	<5	2	<0.5	<5	14	<2	130	52	0.44
1807	1206	1.5	12	26	35	102	<5	2	<0.5	<5	39	<2	200	20	2.6
1808	438	0.6	4	11	28	66	<5	2	<0.5	<5	38	<2	255	16	5.6
1809	108	0.1	<1	4	13	37	<5	3	<0.5	<5	13	<2	140	81	0.47
1810	1571	1.9	11	9	48	109	<5	2	<0.5	<5	36	<2	90	15	0.38
1811	1718	2.0	11	7	85	70	<5	2	<0.5	<5	26	<2	60	11	0.28
1812	3016	1.4	12	10	52	166	<5	2	<0.5	<5	44	<2	150	28	0.14
1813	910	2.8	15	7	65	161	<5	2	<0.5	<5	35	<2	130	12	0.17
1814	373	1.0	6	7	37	68	<5	2	<0.5	<5	26	<2	105	8	3.3
1815	199	0.8	4	5	25	54	<5	1	<0.5	<5	21	<2	120	7	12.0
1816	1703	2.3	25	11	46	92	<5	2	<0.5	<5	26	<2	75	8	2.5
1817	104	1.0	6	7	64	64	<5	3	<0.5	<5	22	<2	120	9	8.3
1818	15	0.1	<1	1	11	24	<5	3	<0.5	<5	6	<2	120	12	33.0
1819	137	0.7	3	11	34	43	<5	4	0.5	<5	14	<2	100	17	8.3
1820	85	0.3	1	4	19	36	<5	2	<0.5	<5	14	<2	86	5	2.6

APPENDIX IV

ANALYTICAL REPRODUCIBILITY

Sample Number	Mn ppm	Fe %	Co ppm	Ni ppm	Cu ppm	Zn ppm	As ppm	Mo ppm	Ag ppm	Sb ppm	Pb ppm	Bi ppm	Hg ppb	*K* micro-mhos/cm	H^+ ppm
1758	430	1.4	143	83	271	881	<5	2	0.5	<5	35	<2	85	172	5.5
1759	312	2.0	53	48	417	328	<5	2	<0.5	<5	30	<2	90	56	1.1
Reproducibility	±16%	±18%	±46%	±27%	±21%	±46%	-	-	-	-	±8%	-	±3%	±51%	±67%
1769	948	0.5	14	23	53	397	<5	2	<0.5	<5	18	<2	125	76	0.09
1770	17140	0.3	49	20	75	417	<5	3	<0.5	<5	32	<2	355	98	0.13
Reproducibility	±90%	±25%	±56%	±7%	±17%	±2%	-	-	-	-	±28%	-	±48%	±13%	±18%
1785	371	0.5	4	9	107	191	42	2	<0.5	<5	32	<2	375	39	0.7
1786	665	0.4	3	6	44	99	56	2	<0.5	<5	28	<2	305	68	0.6
Reproducibility	±28%	±11%	±14%	±20%	±42%	±32%	±14%	-	-	-	±7%	-	±10%	±27%	±8%
1797	823	1.5	10	13	100	75	<5	1	<0.5	<5	32	<2	115	19	1.3
1798	789	1.9	14	14	96	129	<5	2	<0.5	<5	38	<2	105	12	0.9
Reproducibility	±2%	±12%	±17%	±4%	±2%	±26%	-	-	-	-	±9%	-	±5%	±23%	±18%
1803	37	0.4	2	5	36	53	<5	3	<0.5	<5	14	<2	40	60	12
1804	44	0.4	2	6	25	33	<5	2	<0.5	<5	17	<2	20	39	9
Reproducibility	±9%	±0%	±0%	±9%	±18%	±23%	-	-	-	-	±10%	-	±33%	±21%	±14%
1815	199	0.8	4	5	25	54	<5	1	<0.5	<5	21	<2	120	7	12
1816	1703	2.3	25	11	46	92	<5	2	<0.5	<5	26	<2	75	8	2.5
Reproducibility	±79%	±48%	±72%	±38%	±30%	±26%	-	-	-	-	±11%	-	±23%	±7%	±66%
Average Reproducibility	±37%	±19%	±34%	±18%	±22%	±26%	±14%	-	-	-	±12%	-	±20%	±24%	±32%

Overall
Average Reproducibility = ±23%

APPENDIX IV (Cont'd)

COMPARISON OF ANALYTICAL RESULTS FOR BONDAR-CLEGG & CO. LTD.AND MANITOBA ENERGY AND MINES ANALYTICAL LABORATORY

Sample Number	Lab[1]	Cu ppm	Ni ppm	Zn ppm	Co ppm	Mn ppm	Fe %
1758	B-C	271	83	881	143	430	1.4
	EM	314	98	890	167	420	1.125
1759	B-C	417	48	328	53	312	2.0
	EM	480	58	357	62	319	2.020
1769	B-C	53	23	397	14	948	0.5
	EM	59	27	407	18	910	0.325
1770	B-C	75	20	417	49	17140	0.3
	EM	77	24	460	58	17100	0.280
1785	B-C	107	9	191	4	371	0.5
	EM	68	13	186	2	430	0.370
1786	B-C	44	6	99	3	665	0.4
	EM	42	5	112	6	670	0.390
1797	B-C	100	13	75	10	823	1.5
	EM	164	14	91	14	910	1.935
1798	B-C	96	14	129	14	789	1.9
	EM	132	17	138	22	870	2.300
1803	B-C	36	5	53	2	37	0.4
	EM	39	4	49	4	36	0.355
1804	B-C	25	6	33	2	44	0.4
	EM	26	2	44	4	42	0.325
1815	B-C	25	5	54	4	199	0.8
	EM	33	6	75	9	247	0.900
1816	B-C	46	11	92	25	1703	2.3
	EM	57	10	115	36	1900	2.750

[1]B-C - Bondar-Clegg & Co. Ltd. performed the analysis.
EM - Manitoba Energy and Mines Analytical Laboratory performed the analysis.

APPENDIX V: HISTOGRAMS

Mn (ppm)

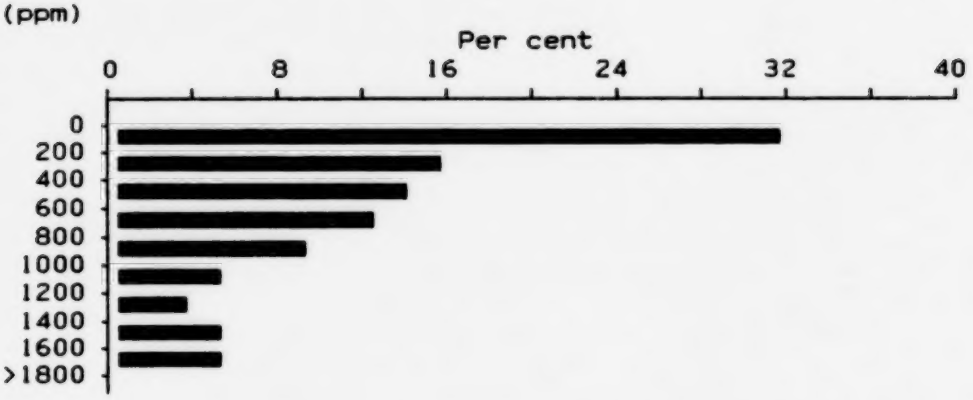

Fe (%)

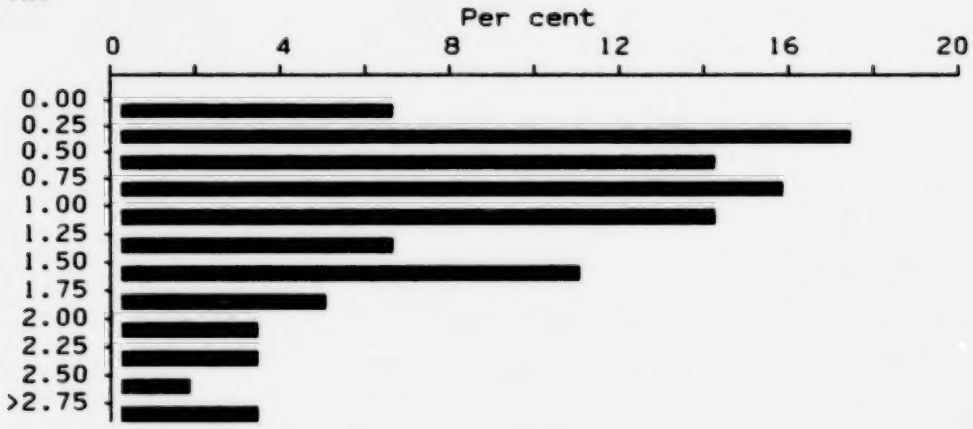

Co (ppm)

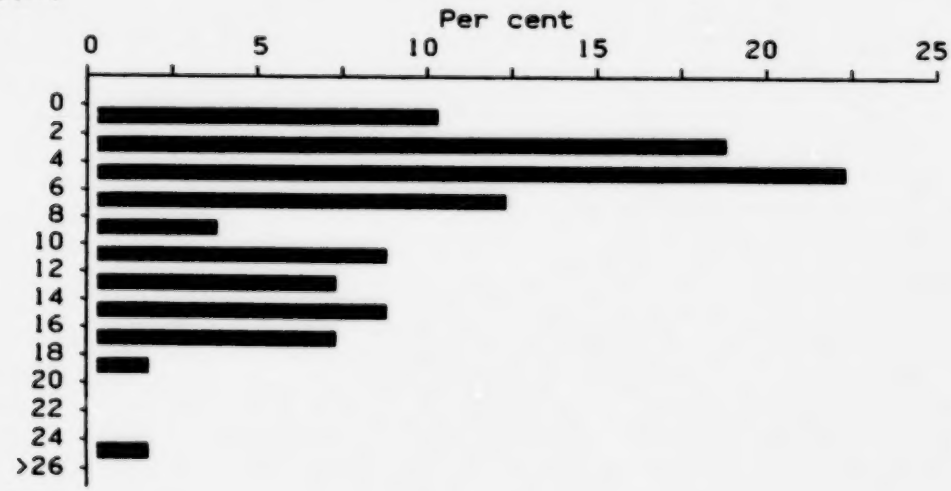

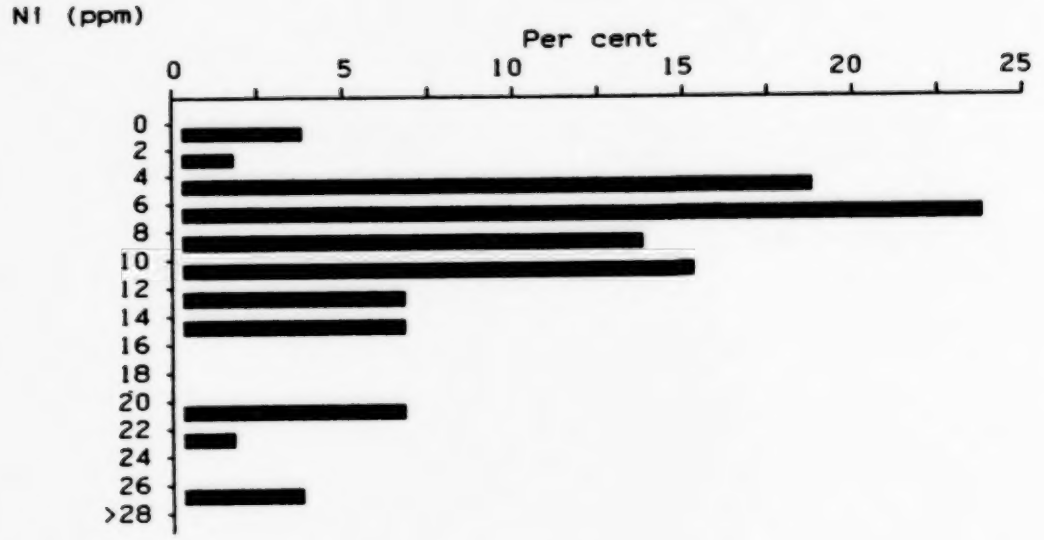
Ni (ppm)
Per cent
0
5
10
15
20
25
0
2
4
6
8
10
12
14
16
18
20
22
24
26
>28

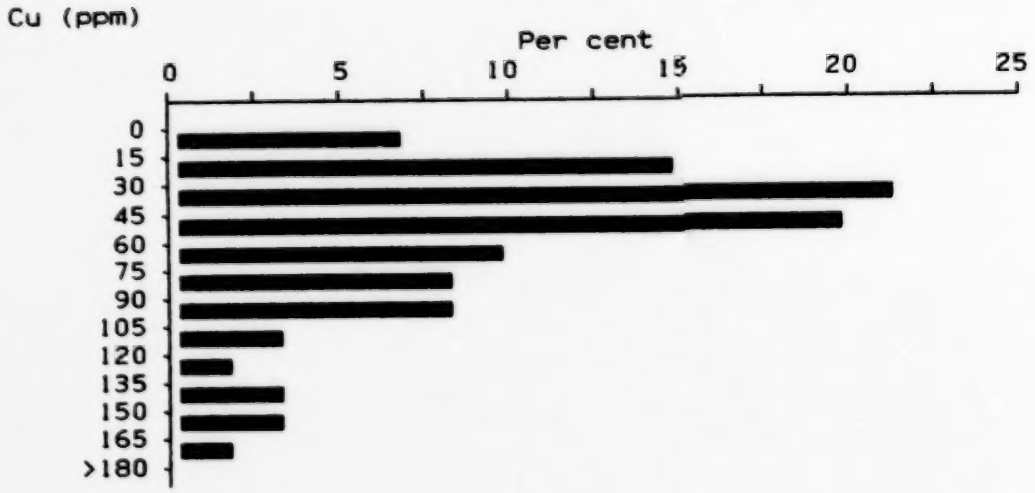
Cu (ppm)
Per cent
0
5
10
15
20
25
0
15
30
45
60
75
90
105
120
135
150
165
>180

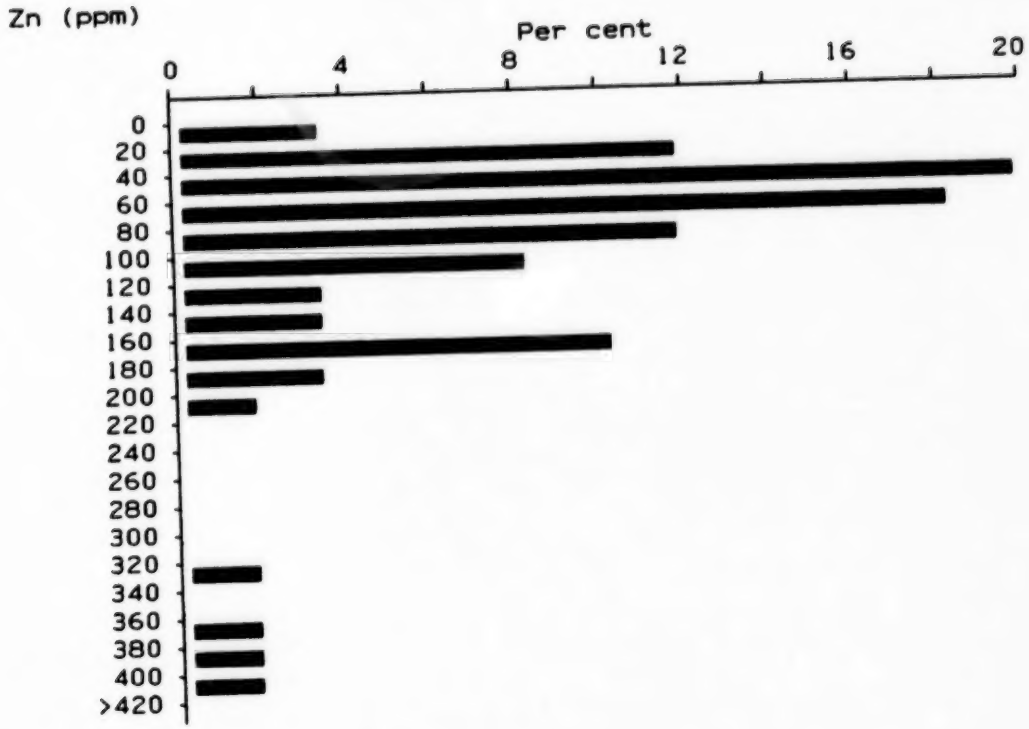
Zn (ppm)
Per cent
0
4
8
12
16
20
0
20
40
60
80
100
120
140
160
180
200
220
240
260
280
300
320
340
360
380
400
>420

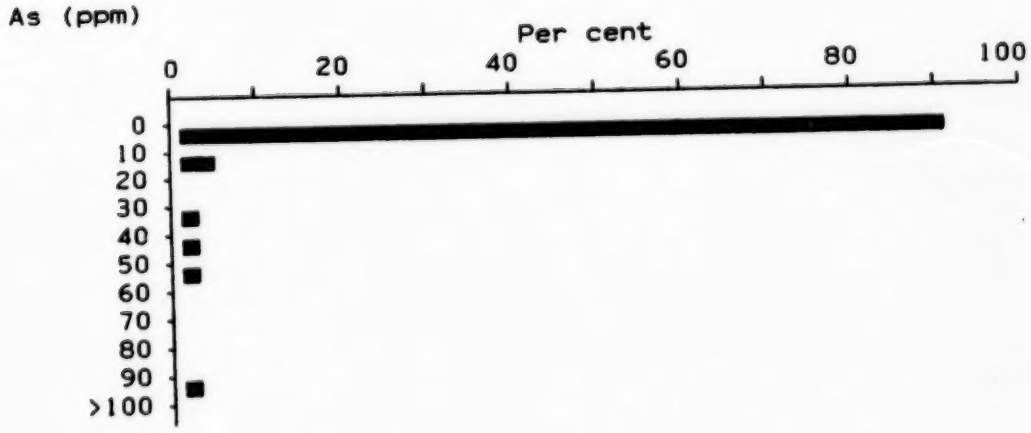
As (ppm)
Per cent
0
20
40
60
80
100
0
10
20
30
40
50
60
70
80
90
>100

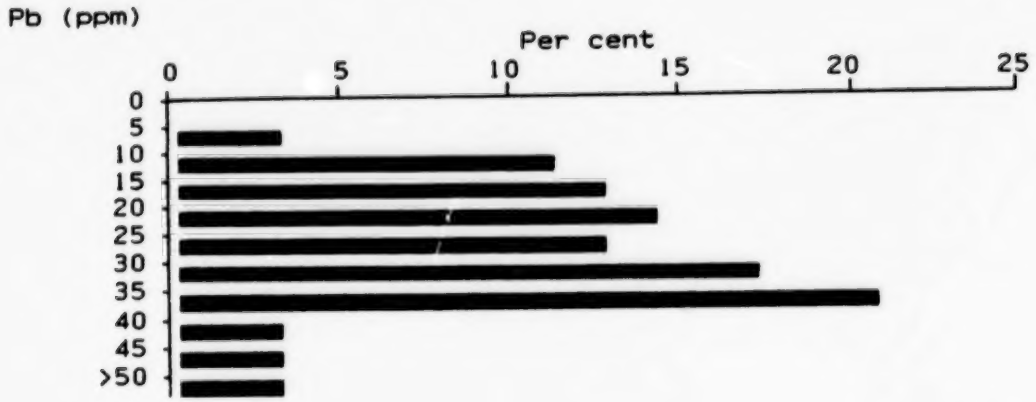
Pb (ppm)
Per cent
0
5
10
15
20
25
0
5
10
15
20
25
30
35
40
45
>50

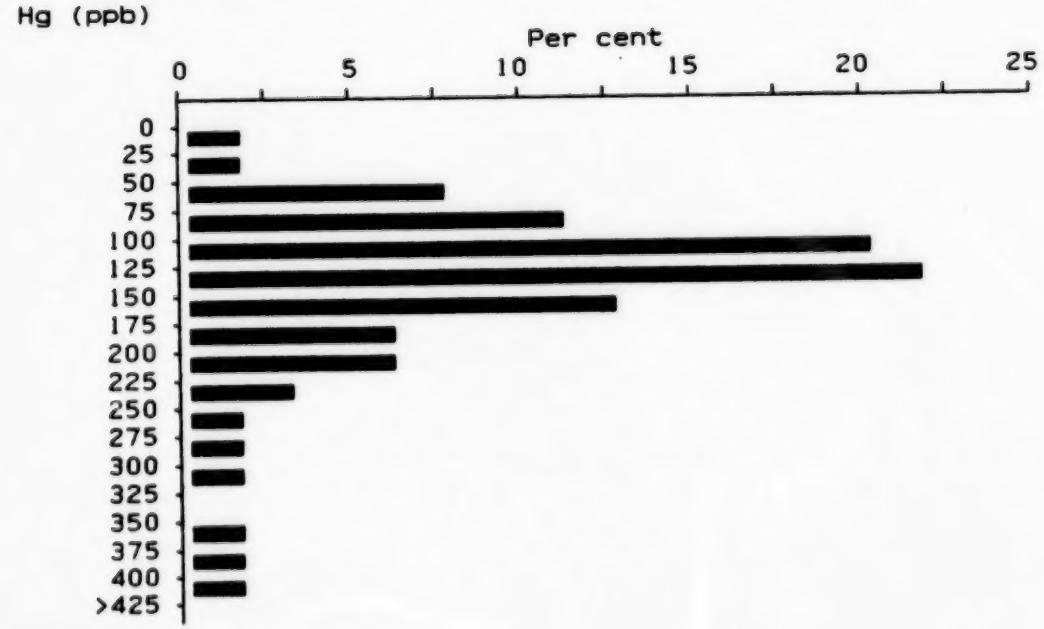
Hg (ppb)
Per cent
0
5
10
15
20
25
0
25
50
75
100
125
150
175
200
225
250
275
300
325
350
375
400
>425

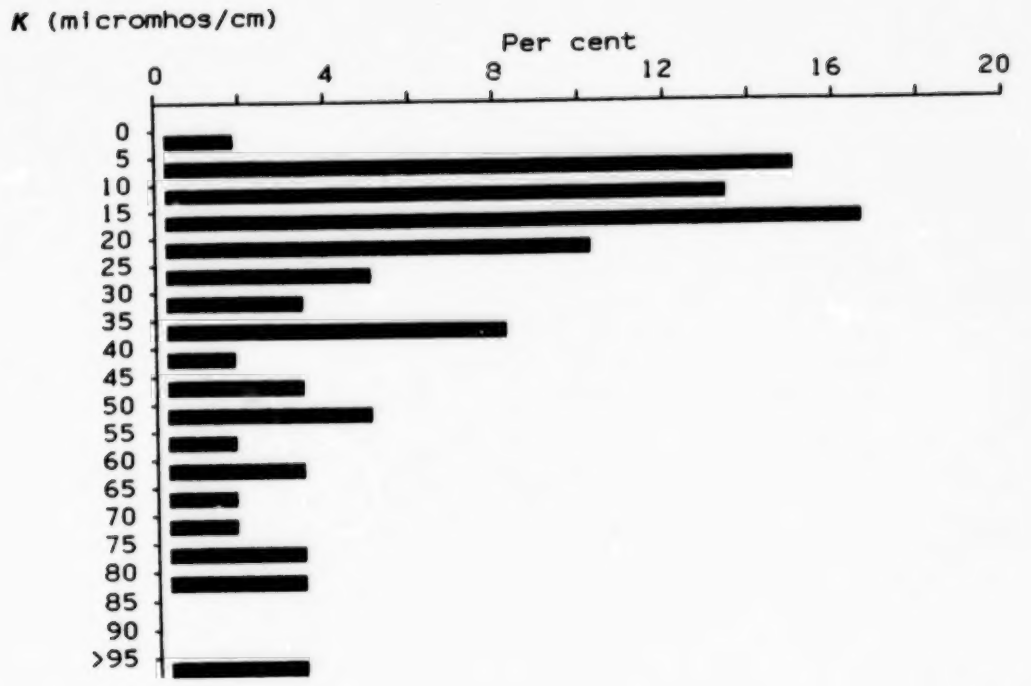
K (micromhos/cm)
Per cent
0
4
8
12
16
20
0
5
10
15
20
25
30
35
40
45
50
55
60
65
70
75
80
85
90
>95

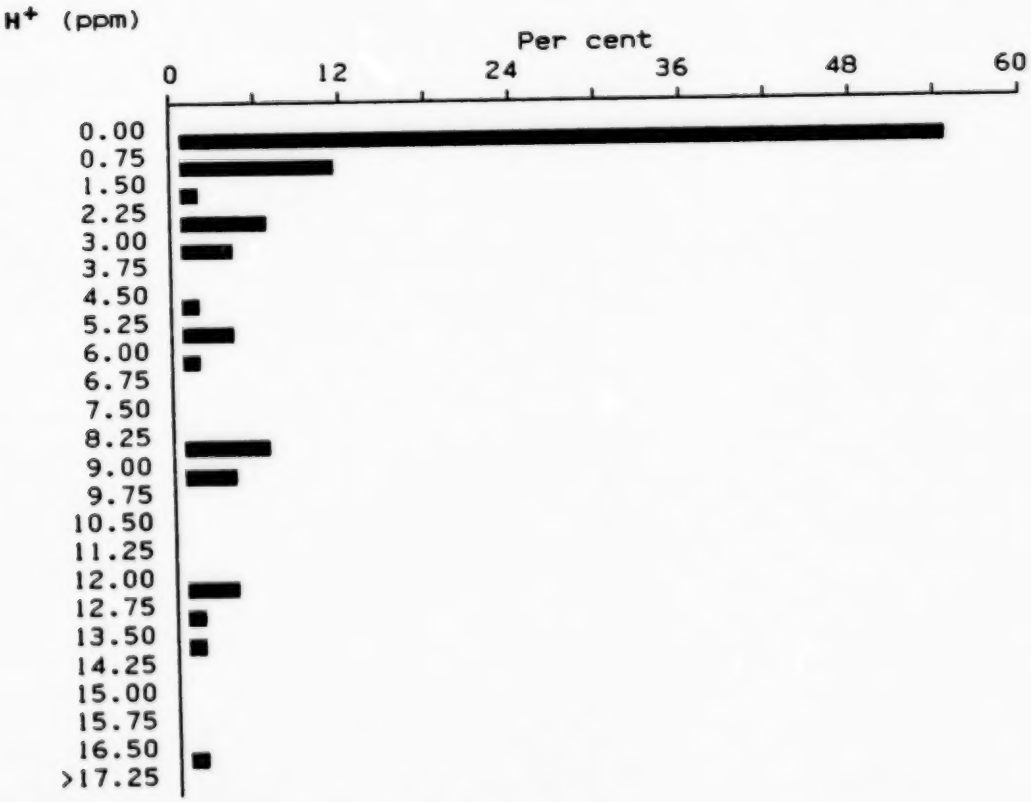
H+ (ppm)
Per cent
0
12
24
36
48
60
0.00
0.75
1.50
2.25
3.00
3.75
4.50
5.25
6.00
6.75
7.50
8.25
9.00
9.75
10.50
11.25
12.00
12.75
13.50
14.25
15.00
15.75
16.50
>17.25